

Precise Unbiased Estimation in Randomized Experiments using Auxiliary Observational Data

Johann A. Gagnon-Bartsch^{*1}, Adam C. Sales^{*2}, Edward Wu¹, Anthony F. Botelho³, John A. Erickson³, Luke W. Miratrix⁴, and Neil T. Heffernan³

¹University of Michigan, Department of Statistics

²University of Texas, Austin, College of Education

³Worcester Polytechnic Institute, Learning Sciences and Technologies

⁴Harvard University, School of Education

May 11, 2021

Abstract

Randomized controlled trials (RCTs) are increasingly prevalent in education research, and are often regarded as a gold standard of causal inference. Two main virtues of randomized experiments are that they (1) do not suffer from confounding, thereby allowing for an unbiased estimate of an intervention’s causal impact, and (2) allow for design-based inference, meaning that the physical act of randomization largely justifies the statistical assumptions made. However, RCT sample sizes are often small, leading to low precision; in many cases RCT estimates may be too imprecise to guide policy or inform science. Observational studies, by contrast, have strengths and weaknesses complementary to those of RCTs. Observational studies typically offer much larger sample sizes, but may suffer confounding. In many contexts, experimental and observational data exist side by side, allowing the possibility of integrating “big observational data” with “small but high-quality experimental data” to get the best of both. Such approaches hold particular promise in the field of education, where RCT sample sizes are often small due to cost constraints, but automatic collection of observational data, such as in computerized educational technology applications, or in state longitudinal data systems (SLDS) with administrative data on hundreds of thousand of students, has made rich, high-dimensional observational data widely available. We outline an approach that allows one to employ machine learning algorithms to learn from the observational data, and use the resulting models to improve precision in randomized experiments. Importantly, there is no requirement that the machine learning models

*These authors contributed equally.

are “correct” in any sense, and the final experimental results are guaranteed to be exactly unbiased. Thus, there is no danger of confounding biases in the observational data leaking into the experiment.

1 Introduction

Randomized controlled trials (RCTs) are famously free of confounding bias. Indeed, a class of estimators, often referred to as “design-based” [Schochet, 2015] or “randomization based” [Rosenbaum, 2002] estimate treatment effects without assuming any statistical model other than whatever is implied by the experimental design itself. Design-based statistical estimators are typically guaranteed to be unbiased. Their associated inference—standard errors, hypothesis tests, confidence intervals—also come with guarantees regarding accuracy. In many cases, these apply regardless of the sample size and require only very weak regularity conditions.

While RCTs can reliably provide unbiased estimates, they are often limited in terms of precision. The statistical precision of RCT-based estimates is inherently limited by the RCT’s sample size, which itself is typically subject to a number of practical constraints.

In contrast, large observational datasets can frequently be brought to bear on some of the same questions addressed by an RCT. Analysis of observational data, unlike RCTs, typically requires a number of untestable modeling assumptions, chief among them the assumption of no unmeasured confounding. Consequently, treatment effect estimates from observational data cannot boast the same guarantees to accuracy as estimates from RCTs. That said, in many cases they boast a much larger sample—and, hence, greater precision—than equivalent RCTs.

In many cases, observational and RCT data coexist within the very same database. For instance, covariate and outcome data for a biomedical RCT may be drawn from a database of electronic health records, and that same database may contain equivalent records for patients who did not participate in the study and were not randomized. Along similar lines, covariate and outcome data for an RCT designed to evaluate the impact of an educational intervention might be drawn from a state administrative database, and that database may also contain information on hundreds of thousands of students who did not participate in the RCT. We refer to these individuals, who are non-participants of the RCT but who are in the same database, as the *remnant* from the study [Sales et al., 2018b]. We ask, how can we use the remnant to improve power to detect effects in RCTs?

An example from the field of education is the ASSISTments TestBed [Heffernan and Heffernan, 2014, Ostrow et al., 2016]. ASSISTments is a computer-based learning platform used by over 50,000 students throughout the United States each year for homework and classwork. The TestBed is an A/B testing program designed for conducting education research that runs within ASSISTments, and has been made accessible to third-party education researchers. Using the TestBed, a researcher can propose A/B tests to run within ASSISTments. That is, a researcher may specify two contrasting conditions, such as video- or text-based instructional feedback, and a particular homework topic, such as “Adding Whole Numbers,” or “Factoring

Quadratic Equations.” Then, students working on that topic are individually randomized between the two conditions. The researcher could then compare the relative impact of video- vs. text-based feedback on an outcome variable of interest such as homework completion. The anonymized data associated with the study, consisting of several levels of granularity and rich covariates describing both historical pre-study and within-study student interaction, is made available to the researcher. The Testbed currently hosts over 100 such RCTs, and several of these RCTs have recently been analyzed [Fyfe, 2016, Walkington et al., 2019, McGuire et al., 2017, Koedinger and McLaughlin, 2016].

In the ASSISTments TestBed example, a given RCT is likely to consist of just a few hundred students assigned to a specific homework assignment, limiting statistical power and precision. For instance, in one typical ASSISTments TestBed A/B test, a total of 294 students were randomized between two conditions, leading to a standard error of roughly four percentage points when estimating the effect on homework completion. This standard error is too large to either determine the direction of a treatment effect or rule out clinically meaningful effect sizes. But the ASSISTments database contains data on hundreds of thousands of other ASSISTments users, many of whom may have completed similar homework assignments, or who may have even completed an identical homework assignment but in a previous time period.

This paper outlines an approach to estimate treatment effects in an RCT while incorporating high-dimensional covariate data, large observational remnant data, and machine learning prediction algorithms to improve precision. It does so without compromising the accuracy guarantees of traditional design-based RCT estimators, yielding unbiased point estimates and sampling variance estimates that are conservative in expectation; the approach is design-based, relying only on the randomization within the RCT to make these guarantees. In particular, the method prevents “bias leakage”: bias that might have occurred due to differences between the remnant and the experimental sample, biased or incorrect modeling of covariates, or other data analysis flaws, does not leak into the RCT estimator. We combine recent causal methods for within-RCT covariate adjustment with other methods that have sought to incorporate high dimensional remnant data into RCT estimators. In particular, we focus on the challenge of precisely estimating treatment effects from a set of 33 TestBed experiments [Selent et al., 2016], using prior log data from experimental participants and non-participants in the ASSISTments system.

The nexus of machine learning and causal inference has recently experienced rapid and exciting development. This has included novel methods to analyze observational studies [e.g., Diamond and Sekhon, 2013], to estimate subgroup effects [e.g., Duivesteyn et al., 2017, Künzel et al., 2018], or to optimally allocate treatment (e.g., Rzepakowski and Jaroszewicz [2012], Zhao and Heffernan [2017]). Other developments share our goal, i.e., improving the precision of average treatment effect estimates from RCTs. These include the flexible approaches of Aronow and Middleton [2013], Wager et al. [2016], and Chernozhukov et al. [2018], all of which can incorporate arbitrary prediction methods, Bloniarz et al. [2016], which uses the Lasso regression estimator [Tibshirani, 1996] to analyze experiments [also see Belloni et al., 2014], and the Targeted Learning framework [Van der Laan and Rose, 2011,

Gruber and van der Laan, 2010, Rosenblum and Van Der Laan, 2010, Steingrimsson et al., 2017], which combines ensemble machine-learning with semiparametric maximum likelihood estimation.

A large literature has explored the possibility of improving precision in RCTs by pooling the controls in the RCT with historical controls from observational datasets or from other similar RCTs. This literature dates back at least to Pocock [1976]; for reviews see, e.g., Viele et al. [2014] and Lim et al. [2018]. Much of this work uses a Bayesian framework, although frequentist approaches exist as well [Yuan et al., 2019]. In many of these methods biases can be arbitrary large depending on the choice of historical controls.

More recent efforts have sought to exploit large observational datasets in the analysis of RCTs, also with the goal of improving precision, in other ways. These include Deng et al. [2013], which uses a variant of the survey regression estimator, combined with covariates drawn from pre-experimental data, to reduce standard errors from online A/B tests; Aronow and Middleton [2013], which proposes a class of design-based unbiased estimators and suggests fitting models to auxiliary datasets; Peysakhovich and Lada [2016], which uses non-experimental time-series data to estimate individual treatment effects in order to improve experimental estimates of subgroup effects; Gui [2020], which uses the RCT to de-bias a broken IV estimate obtained from observational data and then further combines this estimate with an independent RCT-based estimate to improve overall efficiency, and which notably is complementary to many of the other methods mentioned here; Ilse et al. [2021], which reduces the space of latent confounding variables in a structural causal model, and Oppen [2021], which develops a variant of the sample-splitting estimator that we review below, and suggests a role for auxiliary data as well.

Other literature has sought to combine experimental and observational data for other purposes, including improving the external validity of RCTs, generalizing the results of RCTs to other populations and also other outcome variables, as well as improving the design of RCTs, among other goals [Hartman et al., 2015, Rothenhäusler, 2020, Rosenman and Owen, 2021, Rosenman et al., 2020, 2018, Athey et al., 2020, Kallus et al., 2018]. For reviews, see Degtiar and Rose [2021], Colnet et al. [2020], Kaizar [2015], Verde and Ohmann [2015]. A parallel literature in survey methodology discusses the possibility of combining probability and nonprobability samples in order to increase precision, especially for small area estimation [Särndal et al., 2003, Breidt et al., 2005, Opsomer et al., 2007, Wang and Wang, 2011, Goga and Ruiz-Gazen, 2014, Breidt and Opsomer, 2017, Erciulescu et al., 2019, 2020, Dagdoug et al., 2020, McConville et al., 2020].

In this paper, our goal is to estimate the average treatment effect within the RCT, and our focus is on using observational data to improve the precision of the estimate. Our approach may be summarized as “first, do no harm,” meaning that we prioritize retaining the advantages of randomized experiments highlighted above. In particular, we seek to ensure that our method (1) does not introduce any bias, (2) will not harm precision, and ideally will improve precision, and (3) does not require any additional statistical assumptions beyond those typically made in design-based analysis of RCTs.

The paper is organized as follows. Section 2 reviews background material, including

design-based RCT analysis and covariate adjustment. Section 3 discusses incorporating remnant data, and presents our main methodological contribution. In Section 4 we apply the method to estimate treatment effects in the 33 TestBed experiments. Section 5 concludes.

2 Methodological Background

2.1 Causal Inference from Experiments

Consider a randomized experiment to estimate the average effect of a binary treatment T on an outcome Y . There are N subjects, indexed by $i = 1, \dots, N$. Let $T_i = 1$ if subject i is assigned to treatment, and $T_i = 0$ if control. Let $\mathcal{T} = \{i \mid T_i = 1\}$ and $\mathcal{C} = \{i \mid T_i = 0\}$, and let $n_t = |\mathcal{T}|$ and $n_c = |\mathcal{C}|$.

Following Neyman [1923] and Rubin [1974], let potential outcomes y_i^t and y_i^c represent the outcome value Y_i that i would have exhibited if he or she had (perhaps counterfactually) been assigned to treatment or control, respectively. Observed outcomes are a function of treatment assignment and potential outcomes:

$$Y_i = T_i y_i^t + (1 - T_i) y_i^c$$

Define the treatment effect for i as $\tau_i = y_i^t - y_i^c$. Our goal will be to estimate the average treatment effect (ATE), $\bar{\tau} \equiv \sum_i \tau_i / N = \bar{y}^t - \bar{y}^c$, where $\bar{y}^t = \sum_{i=1}^N y_i^t / N$ is the mean of y^t over all N units in the experiment and \bar{y}^c is defined similarly.

If both y_i^c and y_i^t were known for each subject i , statistical modeling would be unnecessary—researchers could calculate $\bar{\tau}$ exactly, without error, by simply averaging observed τ . In practice, we never observe both y_i^c and y_i^t . Instead, we rely on the experimental setup to estimate and infer causation. Since the treatment and control groups are each random samples of the N participants, survey sampling literature provides design-based unbiased estimators of \bar{y}^t and \bar{y}^c based on observed Y and the known distribution of T . These estimators, and their associated inference, depend only on the experimental design, and not on modeling assumptions. The survey sample structure of randomized experiments allows us to infer counterfactual potential outcomes (at least on average) and estimate $\bar{\tau}$ as if τ_i were available for each i , albeit with sampling error.

We will use this framework to analyze the 33 TestBed experiments. These experiments are examples of “Bernoulli experiments,” in which each T_i is an independent Bernoulli trial: $\mathbb{P}(T_i = 1) = p$, with $0 < p < 1$, and $T_i \perp T_j$ if $i \neq j$. In the TestBed experiments, $p = 1/2$. Estimation and inference about $\bar{\tau}$ is based on the observed values of Y and T , and the known value of p .

We will now introduce some statistical elements that we will use as the ingredients for our approach. Let $M_i = T_i y_i^c + (1 - T_i) y_i^t$ denote i ’s unobserved counterfactual outcome—when i is treated, $M_i = y_i^c$ and when i is in the control condition $M_i = y_i^t$. Then i ’s treatment effect may be expressed as $\tau_i = (-1)^{T_i} (M_i - Y_i)$, i.e., $\tau_i = M_i - Y_i$ if i is in the control group, or $\tau_i = Y_i - M_i$ if i is in the treatment group. Although M_i is, by definition, unobserved, it

plays a central role in causal inference; its expectation,

$$m_i \equiv \mathbb{E}M_i = py_i^c + (1-p)y_i^t$$

will also play a prominent role. Note that m_i is a weighted average of subject i 's potential outcomes.

Let

$$U_i = \begin{cases} \frac{1}{p} & T_i = 1 \\ -\frac{1}{1-p} & T_i = 0 \end{cases}$$

be subject i 's signed inverse probability weights; U_i is merely a rescaled treatment indicator. Note that $\mathbb{E}U_i = 0$, and $\mathbb{E}U_iY_i = \tau_i$. To see the latter, note that when $T = 1$, with probability p , $Y_i = y_i^t$ and $U_iY_i = y_i^t/p$; when $T = 0$, with probability $1-p$, $U_iY_i = -y_i^c/(1-p)$. Thus U_iY_i may be thought of as an unbiased estimate of τ_i , and $\hat{\tau}^{\text{IPW}} \equiv \sum_i U_iY_i/N$ is an unbiased estimate of $\bar{\tau}$. Note $\hat{\tau}^{\text{IPW}}$ is identical to the ‘‘Horvitz-Thompson’’ estimator of Aronow and Middleton [2013]

$$\hat{\tau}^{\text{IPW}} = \frac{1}{N} \sum_{i \in \mathcal{T}} \frac{Y_i}{p} - \frac{1}{N} \sum_{i \in \mathcal{C}} \frac{Y_i}{1-p} \quad (1)$$

since it is the difference between the Horvitz-Thomson estimates of \bar{y}^t and \bar{y}^c [Horvitz and Thompson, 1952].

The sampling variance of $\hat{\tau}^{\text{IPW}}$ proceeds from the same principals. The variance of U_iY_i is

$$\mathbb{V}(U_iY_i) = \left(y_i^t \sqrt{\frac{1-p}{p}} + y_i^c \sqrt{\frac{p}{1-p}} \right)^2 = \frac{m_i^2}{p(1-p)} \quad (2)$$

and $\mathbb{V}(\hat{\tau}^{\text{IPW}}) = \sum_i m_i^2/[N^2p(1-p)]$ because treatment assignments are independent. Note that because y_i^t and y_i^c are never simultaneously observed, $\mathbb{V}(\hat{\tau}^{\text{IPW}})$ is not identified. However, $\hat{\mathbb{V}}(\hat{\tau}^{\text{IPW}}) = \sum_i U_i^2 Y_i^2/N^2$ is an upper bound, i.e., $\mathbb{E}\hat{\mathbb{V}}(\hat{\tau}^{\text{IPW}}) \geq \mathbb{V}(\hat{\tau}^{\text{IPW}})$. (See Aronow and Middleton [2013] for equivalent expressions for more general experimental designs.)

Strangely, $\hat{\tau}^{\text{IPW}}$ and $\mathbb{V}(\hat{\tau}^{\text{IPW}})$ are not translation-independent, i.e., adding a constant to each Y changes both the value of $\hat{\tau}^{\text{IPW}}$ and $\mathbb{V}(\hat{\tau}^{\text{IPW}})$ without changing the estimand $\bar{\tau}$. The more popular simple ‘‘difference-in-means’’ estimator [Neyman, 1923],

$$\hat{\tau}^{\text{DM}} = \frac{1}{n_t} \sum_{i \in \mathcal{T}} Y_i - \frac{1}{n_c} \sum_{i \in \mathcal{C}} Y_i = \bar{Y}_{\mathcal{T}} - \bar{Y}_{\mathcal{C}} \quad (3)$$

and its associated variance estimator

$$\hat{\mathbb{V}}(\hat{\tau}^{\text{DM}}) = \frac{S^2(Y_{\mathcal{C}})}{n_c} + \frac{S^2(Y_{\mathcal{T}})}{n_t} \quad (4)$$

where $S^2(Y_{\mathcal{C}}) = \sum_{i \in \mathcal{C}} (Y_i - \bar{Y}_{\mathcal{C}})^2/(n_c - 1)$ is the sample variance of the control group and $S^2(Y_{\mathcal{T}})$ is defined similarly, do not have this undesirable property. Our presentation here focuses on $\hat{\tau}^{\text{IPW}}$ as a jumping-off point for subsequent methodological development, but $\hat{\tau}^{\text{DM}}$ will also play a prominent role.

2.2 Design-Based Covariate Adjustment

The reason for error when estimating τ is our inability to observe counterfactual potential outcomes M . As we have seen, randomized trials, coupled with design-based estimators like $\hat{\tau}^{\text{IPW}}$, use comparison groups and survey sampling theory to implicitly fill in this missing information. Baseline covariates—a vector \mathbf{x}_i of data for subject i gathered prior to treatment randomization—may potentially help us improve upon this strategy. Suppose a researcher has constructed algorithms $\hat{y}^c(\cdot)$ and $\hat{y}^t(\cdot)$ designed to impute y^c and y^t , respectively, from \mathbf{x} . Then $\hat{M}_i = T_i \hat{y}^c(\mathbf{x}_i) + (1 - T_i) \hat{y}^t(\mathbf{x}_i)$ is an imputation of i 's missing counterfactual outcome, and the researcher may estimate τ_i as $(-1)^{T_i}(\hat{M}_i - Y_i)$. In general, the bias of algorithms such as $\hat{y}^c(\cdot)$ and $\hat{y}^t(\cdot)$ will be unknown without further assumptions, so these effect estimates may be inadvisable. On the other hand, imperfect or potentially biased imputations of potential outcomes can, *when combined with randomization*, yield substantial benefits.

The approach we will take to combining covariate adjustment with randomization follows Wu and Gagnon-Bartsch [2018], as will its presentation here. It has antecedents in Robins et al. [1994], Scharfstein et al. [1999], Robins [2000], Rosenbaum [2002], Bang and Robins [2005], van der Laan and Rubin [2006], Tsiatis et al. [2008], Moore and van der Laan [2009], Van der Laan and Rose [2011], Aronow and Middleton [2013], Belloni et al. [2014], Wager et al. [2016], and Chernozhukov et al. [2018], among others.

In a Bernoulli experiment, note that

$$\begin{aligned} U_i(Y_i - m_i) &= \begin{cases} \frac{1}{p}(y_i^t - py_i^c - (1-p)y_i^t) & T_i = 1 \\ -\frac{1}{1-p}(y_i^c - py_i^c - (1-p)y_i^t) & T_i = 0 \end{cases} \\ &= \begin{cases} \frac{p(y_i^t - y_i^c)}{p} & T_i = 1 \\ \frac{(1-p)(y_i^t - y_i^c)}{1-p} & T_i = 0 \end{cases} \\ &= \tau_i \end{aligned}$$

and this therefore suggests using imputations $\hat{y}^c(\mathbf{x}_i)$ and $\hat{y}^t(\mathbf{x}_i)$ to estimate m_i as $\hat{m}_i = p\hat{y}^c(\mathbf{x}_i) + (1-p)\hat{y}^t(\mathbf{x}_i)$, and then estimating τ_i as

$$\hat{\tau}_i \equiv U_i(Y_i - \hat{m}_i).$$

It turns out that $\hat{\tau}_i$ is unbiased if algorithms $\hat{y}^c(\cdot)$ and $\hat{y}^t(\cdot)$ are constructed in such a way that

$$\{\hat{y}^c(\mathbf{x}_i), \hat{y}^t(\mathbf{x}_i)\} \perp\!\!\!\perp T_i. \quad (5)$$

Since $\mathbf{x}_i \perp\!\!\!\perp T_i$ by design, (5) is tantamount to requiring that T_i , and variables such as Y_i that depend on T_i , play no role in constructing algorithms $\hat{y}^c(\cdot)$ and $\hat{y}^t(\cdot)$. Then, under (5),

$$\mathbb{E}(\hat{\tau}_i) = \mathbb{E}(U_i Y_i) - \mathbb{E}(U_i \hat{m}_i) = \mathbb{E}(U_i Y_i) - \mathbb{E}(U_i) \mathbb{E}(\hat{m}_i) = \mathbb{E}(U_i Y_i) = \tau_i$$

where we use the facts that $\mathbb{E}(U_i) = 0$ and $\mathbb{E}(U_i Y_i) = \tau_i$. Finally, define the ATE estimate:

$$\hat{\tau} = \frac{1}{N} \sum_{i=1}^N \hat{\tau}_i = \frac{1}{N} \sum_{i \in \mathcal{T}} \frac{Y_i - \hat{m}_i}{p} - \frac{1}{N} \sum_{i \in \mathcal{C}} \frac{Y_i - \hat{m}_i}{1-p} \quad (6)$$

The unbiasedness of $\hat{\tau}$ for $\bar{\tau}$ follows from the unbiasedness of each of its summands, $\hat{\tau}_i$ for τ_i .

Crucially, this unbiasedness holds even if $\hat{y}^c(\mathbf{x}_i)$ and $\hat{y}^t(\mathbf{x}_i)$ are biased; algorithms $\hat{y}^c(\cdot)$ and $\hat{y}^t(\cdot)$ need not be unbiased, consistent, or correct in any sense. As long as $\hat{y}^c(\mathbf{x}_i)$ and $\hat{y}^t(\mathbf{x}_i)$ are constructed to be independent of T_i , then $\hat{\tau}_i$ will be unbiased. The same cannot be said for regression-based covariate adjustment, the common technique of regressing Y on T and \mathbf{x} [Freedman, 2008].

Compare the estimate $\hat{\tau}$ given in (6) to the estimate $\hat{\tau}^{\text{IPW}}$ given in (1). The only difference is that Y_i in (6) has been replaced by $Y_i - \hat{m}_i$ in (1). The goal of this covariate adjustment is to improve precision—we are residualizing our outcomes, in effect, to reduce variation. Its success in this regard depends on the predictive accuracy of $\hat{y}^c(\mathbf{x}_i)$ and $\hat{y}^t(\mathbf{x}_i)$. The variance of $\hat{\tau}_i$ depends on \hat{m}_i and is given by

$$\mathbb{V}(\hat{\tau}_i | \hat{m}_i) = \frac{(\hat{m}_i - m_i)^2}{p(1-p)}. \quad (7)$$

Compared with (2), (7) replaces m_i with $\hat{m}_i - m_i$ —that is, replaces potential outcomes with their residuals. Accurate imputations of y_i^c and y_i^t , and hence of \hat{m}_i , yield precise estimation of τ_i . On the other hand, inaccurate imputations, i.e., when $(\hat{m}_i - m_i)^2$ is greater than m_i^2 , will decrease precision—though, again, without causing bias.

2.3 Sample Splitting

Successful covariate adjustment requires imputations $\hat{y}^c(\mathbf{x}_i)$ and $\hat{y}^t(\mathbf{x}_i)$ that are accurate and independent of T_i . To satisfy the independence condition, i 's observed outcome Y_i , which is a function of T_i , cannot play a role in the construction of the algorithms $\hat{y}^c(\cdot)$ and $\hat{y}^t(\cdot)$; they must be trained using other data.

This may be achieved by sample splitting, also referred to in this context as cross-estimation or cross-fitting. In a Bernoulli experiment, rather than fitting global imputation algorithms $\hat{y}^t(\cdot)$ and $\hat{y}^c(\cdot)$ (which would violate 5), fit a separate set of imputation models $\hat{y}_{-i}^t(\cdot)$ and $\hat{y}_{-i}^c(\cdot)$ for each experimental participant i , using data from the other participants. In other words, for each i , one first drops observation i , and then use the remaining $N - 1$ observations to construct imputation models for the control and treatment potential outcomes, denoted $\hat{y}_{-i}^c(\cdot)$ and $\hat{y}_{-i}^t(\cdot)$, respectively. These models may be fit by any method, for example linear regression or random forests [Breiman, 2001] (which, conveniently, automatically provides out-of-bag predictions for each subject). In particular, methods that allow for regularization to prevent overfitting may be used.

In this leave-one-out context,

$$\hat{m}_i = p\hat{y}_{-i}^c(\mathbf{x}_i) + (1-p)\hat{y}_{-i}^t(\mathbf{x}_i)$$

and the estimated average treatment effect is then again given by $\hat{\tau}^{\text{SS}} = \sum_i \hat{\tau}_i / N$ as in (6), and where the superscript denotes “sample splitting.” Note that in a Bernoulli experiment $\hat{m}_i \perp T_i$ due to the fact that \hat{m}_i is computed using \mathbf{x}_i and a model fit without using

observation i . It follows that $\hat{\tau}^{\text{SS}}$ is unbiased. Other randomization designs would call for modifications to the algorithm [e.g. Wu and Gagnon-Bartsch, 2021].

When we wish to explicitly specify the covariates and imputation method that are used within $\hat{\tau}^{\text{SS}}$ we will write $\hat{\tau}^{\text{SS}}[\text{covariates}; \text{imputation method}]$. For example, if we wished to use random forests and all available covariates we would write $\hat{\tau}^{\text{SS}}[\mathbf{x}; \text{RF}]$, or if we wished to use only the fourth covariate and ordinary least squares regression we would write $\hat{\tau}^{\text{SS}}[x_4; \text{OLS}]$. If we wished to ignore the covariates and always set $\hat{m}_i = 0$ we would write $\hat{\tau}^{\text{SS}}[\emptyset; 0]$. Note in particular that $\hat{\tau}^{\text{SS}}[\emptyset; 0] = \hat{\tau}^{\text{IPW}}$.

Building upon (7), and following Wu and Gagnon-Bartsch [2018], the variance of $\hat{\tau}^{\text{SS}}$ may be estimated as follows. Let

$$\hat{E}_c^2 = \frac{1}{n_c} \sum_{i \in \mathcal{C}} [\hat{y}_{-i}^c(\mathbf{x}_i) - y_i^c]^2 \quad (8)$$

be the mean-squared-error of control imputations $\hat{y}^c(\mathbf{x}_i)$ with respect to potential outcomes y^c , and define \hat{E}_t^2 similarly. Note \hat{E}_c^2 and \hat{E}_t^2 are leave-one-out cross validation mean squared errors. The estimated variance is then given by

$$\hat{\mathbb{V}}(\hat{\tau}^{\text{SS}}) = \frac{1}{N} \left[\frac{p}{1-p} \hat{E}_c^2 + \frac{1-p}{p} \hat{E}_t^2 + 2\sqrt{\hat{E}_c^2 \hat{E}_t^2} \right]. \quad (9)$$

This variance estimate will typically be somewhat conservative. This is due to the fact that $\mathbb{V}(\hat{\tau}^{\text{SS}})$ is unidentifiable, because the correlation of the potential outcomes is not estimable, and instead an upper bound is used. This difficulty is not unique to $\hat{\tau}^{\text{SS}}$; as noted in Section 2.1, similar comments apply to $\hat{\tau}^{\text{IPW}}$, and the same is true of $\hat{\tau}^{\text{DM}}$ as well [Neyman, 1923, Aronow et al., 2014].

Note that by (9),

$$\begin{aligned} \hat{\mathbb{V}}(\hat{\tau}^{\text{SS}}) &\leq \frac{\hat{E}_c^2}{N(1-p)} + \frac{\hat{E}_t^2}{Np} \\ &\approx \frac{\hat{E}_c^2}{n_c} + \frac{\hat{E}_t^2}{n_t} \end{aligned} \quad (10)$$

which is similar in form to the variance estimate typically used in a two-sample t -test, namely $\frac{S^2(Y_{\mathcal{C}})}{n_c} + \frac{S^2(Y_{\mathcal{T}})}{n_t}$. In (10), $S^2(Y_{\mathcal{C}})$ and $S^2(Y_{\mathcal{T}})$ are replaced by \hat{E}_c^2 and \hat{E}_t^2 . In other words, the sample variances are replaced by the estimated mean squared errors of the imputations.

A special case occurs when the potential outcomes are imputed by simply taking the mean of the observed outcomes (after dropping observation i). That is, we set

$$\hat{y}_{-i}^c(\mathbf{x}_i) = \frac{1}{|\mathcal{C} \setminus i|} \sum_{j \in \mathcal{C} \setminus i} y_j^c$$

and similarly for $\hat{y}_{-i}^t(\mathbf{x}_i)$. Note that the covariates are simply ignored, and we denote this special case by $\hat{\tau}^{\text{SS}}[\emptyset; \text{mean}]$. It can be shown that $\hat{\tau}^{\text{SS}}[\emptyset; \text{mean}] = \hat{\tau}^{\text{DM}}$, i.e., the sample splitting

estimator using leave-one-out mean imputation is exactly equal to the simple difference-in-means estimator. Moreover, in this special case $\hat{E}_c^2 = \frac{n_c}{n_c-1} S^2(Y_C)$ and $\hat{E}_t^2 = \frac{n_t}{n_t-1} S^2(Y_T)$ and thus the variance estimate given by (10) is nearly identical to the ordinary t -test variance estimate [Wu and Gagnon-Bartsch, 2018].

In short, when using mean imputation for the potential outcomes, the leave-one-out sample splitting procedure essentially simplifies to a standard t -test. The effect estimate is identical, and the variance estimate is nearly identical. This is highly reassuring. Any imputation strategy that improves upon mean imputation in terms of mean squared error will reduce the variance of $\hat{\tau}^{\text{SS}}$ relative to $\hat{\tau}^{\text{DM}}$. Most modern machine learning methods employ some form of regularization to guard against overfitting, and thus typically perform no worse, or at least not substantially worse, than mean-imputation. Thus in practice there is relatively little risk of hurting precision.

3 Incorporating Observational Data

Modern field trials are often conducted within a very data-rich context, in which rich high-dimensional covariate data is automatically, or already, collected for all experiment participants. For instance, in the TestBed experiments, system administrators have access to log data for every problem and skill builder each participating student worked before the onset of the experiment. In other contexts, such as healthcare or education, rich administrative data is often available. In fact, these covariates are available for a much wider population than just the experimental participants—in the TestBed case, there is log data for all ASSISTments users. In other education or healthcare examples, administrative data is often available for every student or patient in the system, not just for those who were randomized to a treatment or control condition. Often, as in the TestBed case, the outcome variable Y is also drawn from administrative or log data. We refer to subjects within the same data system in which the experiment took place—i.e. for whom covariate and outcome data are available—but who were not part of the experiment, as the “remnant” from the experiment. The remnant from a TestBed experiment consists of all ASSISTments users for whom log data is available but who did not participate in the experiment, of whom there are several hundred thousand.

This section will outline our main methodological contribution, a set of unbiased effect estimators that use the remnant to improve precision. The estimators all begin by using the remnant to fit or train a model predicting potential outcomes as a function of covariates, and using that model to impute potential outcomes for units in the experiment. They differ in how they use those imputations, and build on each other. The following subsection discusses a simple residualizing estimator, Section 3.2 discusses sample splitting to improve that estimator, and Section 3.3 discusses incorporating an additional set of covariate-adjustment models fit to data from the experimental subjects themselves.

3.1 Covariate Adjustment Using the Remnant

Clearly, pooling data from the remnant with data from the experiment undermines the randomization. As an alternative, Aronow and Middleton [2013] suggest using an “auxiliary dataset” to choose parameters for imputation models $\hat{y}_{-i}^c(\cdot)$ and $\hat{y}_{-i}^t(\cdot)$ to be used for covariate adjustment. Along those lines, Sales et al. [2018a] proposes remnant-based covariate adjustment: first, use data from the remnant to train an algorithm $\hat{y}^r(\cdot)$ to predict outcomes as a function of covariates. Then apply the trained algorithm to the experimental participants, using their covariates \mathbf{x} to predict their outcomes. That is, for each participant i in the experiment, the analyst would compute $\hat{y}^r(\mathbf{x}_i)$, where $\hat{y}^r(\cdot)$ is trained using only data from the remnant.

It may not be clear precisely what $\hat{y}^r(\mathbf{x}_i)$ predicts. For example, if the experimental condition consists of some specific intervention while the control condition is “business as usual,” and if everyone in the remnant experiences “business as usual,” then we might view $\hat{y}^r(\mathbf{x}_i)$ as an imputation of subject i ’s control potential outcome. If, however, the subjects in the RCT are a non-representative sample of the overall population, then we may not even wish to view $\hat{y}^r(\mathbf{x}_i)$ as an imputation of subject i ’s control potential outcome, and the interpretation of $\hat{y}^r(\mathbf{x}_i)$ is more opaque.

Setting aside this issue for now, covariate adjustment using the remnant may proceed as follows. First, one defines residuals $R_i \equiv Y_i - \hat{y}^r(\mathbf{x}_i)$. These residuals are outcome variables, so R_i has two potential outcomes, r_i^c and r_i^t . If subject i is in control, then $R_i = y_i^c - \hat{y}^r(\mathbf{x}_i) = r_i^c$, and if i is in treatment, then $R_i = y_i^t - \hat{y}^r(\mathbf{x}_i) = r_i^t$. Importantly, note that $\hat{y}^r(\mathbf{x}_i)$ is invariant to treatment assignment, and $\hat{y}^r(\mathbf{x}_i)$ is therefore identical in both the control and treatment conditions. This is because the covariates \mathbf{x} are pre-treatment, and because the function $\hat{y}^r(\cdot)$ is trained on the remnant and therefore unaffected by treatment assignments in the RCT. As a result, residualization leaves the estimand intact, i.e.,

$$r_i^t - r_i^c = [y_i^t - \hat{y}^r(\mathbf{x}_i)] - [y_i^c - \hat{y}^r(\mathbf{x}_i)] = y_i^t - y_i^c = \tau_i.$$

Therefore, the outcome Y may be replaced with the residualized outcome R in any unbiased estimator of the ATE, and the result will be an unbiased estimate of $\bar{\tau}$. For instance, treatment effects may be estimated by replacing Y_i with R_i in the Horvitz-Thompson estimator (1); this is equivalent to $\hat{\tau}$ in (6), with $\hat{m}_i = \hat{y}^r(\mathbf{x}_i)$. Alternatively, treatment effects may be estimated as the simple difference-in-means of R between treatment and control groups, i.e.,

$$\hat{\tau}^{\text{RE}} = \frac{1}{n_t} \sum_{i \in \mathcal{T}} R_i - \frac{1}{n_c} \sum_{i \in \mathcal{C}} R_i = \bar{R}_{\mathcal{T}} - \bar{R}_{\mathcal{C}} \quad (11)$$

and with variance estimator

$$\hat{V}(\hat{\tau}^{\text{RE}}) = \frac{S^2(R_{\mathcal{C}})}{n_c} + \frac{S^2(R_{\mathcal{T}})}{n_t}. \quad (12)$$

In what follows we will refer specifically to (11) as “the remnant estimator.” This estimator (or a slight variant thereof) has been previously suggested in Aronow and Middleton [2013], Deng et al. [2013], and Sales et al. [2018b].

Importantly for practitioners, as long as only remnant data is used, $\hat{y}^r(\cdot)$ may be trained and assessed in any way. This process can be iterative, so that an analyst may train a candidate model, assess its performance (perhaps with k -fold cross-validation), modify the algorithm, and repeat until suitable performance is achieved. Any approach to modeling may be taken, so long as no data from the RCT is used. The problem of post-selection inference, which would be a serious concern if modeling were done instead on the RCT data (especially when the dimension of \mathbf{x} is large and the sample size is small), does not apply here. Moreover, the guarantee that $\hat{\tau}^{\text{RE}}$ is unbiased does *not* require that $\hat{y}^r(\cdot)$ itself be unbiased, consistent, or “correct” in any sense; indeed, as suggested above, it may not even be clear precisely what $\hat{y}^r(\cdot)$ is estimating. However $\hat{y}^r(\cdot)$ is fit to the remnant, the remnant estimator is guaranteed to be exactly unbiased due to the randomization in the RCT.

The goal of using the remnant for covariate adjustment is to improve precision. As noted above, the variance estimate of $\hat{\tau}^{\text{RE}}$ is $S^2(R_{\mathcal{C}})/n_c + S^2(R_{\mathcal{T}})/n_t$, while that of difference-in-means $\hat{\tau}^{\text{DM}}$ is $S^2(Y_{\mathcal{C}})/n_c + S^2(Y_{\mathcal{T}})/n_t$. We therefore desire $S^2(R_{\mathcal{C}}) < S^2(Y_{\mathcal{C}})$ and $S^2(R_{\mathcal{T}}) < S^2(Y_{\mathcal{T}})$. In other words, we wish for $\hat{y}^r(\mathbf{x})$ to capture at least some of the variation in Y , so that R is less variable than Y . This will be achieved in practice when $\hat{y}^r(\cdot)$ does indeed successfully predict outcomes in the RCT.

However, in some cases the remnant estimator may have greater sampling variance than the $\hat{\tau}^{\text{DM}}$. This will be the case if $\hat{y}^r(\cdot)$, trained in the remnant, extrapolates poorly to the experimental sample—for instance, if the distribution of Y conditional on \mathbf{x} differs substantially between the remnant and the RCT. We will see examples of remnant-based covariate adjustment harming precision, sometimes substantially, in Section 4 when we analyze the ASSISTments trials.

That said, the remnant estimator is at least somewhat robust to systematic differences between the remnant and the RCT. For instance, if outcomes in the RCT are systematically shifted from those in the remnant by a fixed constant amount, the remnant estimator can still perform well. In other words, if d is some fixed constant, then replacing $\hat{y}^r(\cdot)$ by $\tilde{y}^r(\cdot) \equiv \hat{y}^r(\cdot) + d$ does not have any impact on the remnant estimator. Both $\bar{R}_{\mathcal{C}}$ and $\bar{R}_{\mathcal{T}}$ will be decreased by d , and thus $\hat{\tau}^{\text{RE}}$ will be unchanged. Moreover, $S^2(R_{\mathcal{C}})$ and $S^2(R_{\mathcal{T}})$ will also both be unchanged. What matters is that $S^2(R_{\mathcal{C}}) < S^2(Y_{\mathcal{C}})$ and $S^2(R_{\mathcal{T}}) < S^2(Y_{\mathcal{T}})$. It is *not* necessary that $\bar{R}_{\mathcal{C}} \approx 0$ or $\bar{R}_{\mathcal{T}} \approx 0$. Note that this property of the remnant estimator also suggests that we need not be overly concerned with whether we regard $\hat{y}^r(\cdot)$ as estimating y^c , y^t , or $\mathbb{E}Y$. If we suppose there is a constant treatment effect, then the remnant estimator would perform equally well if $\hat{y}^r(\cdot)$ is estimating y^c , y^t , or $\mathbb{E}Y$, as these would all simply be shifted versions of one another.

To summarize, the remnant is often much larger than the experimental sample, and may provide fertile ground for fitting outcome models, especially in the presence of rich high-dimensional covariates. Once a reasonably good outcome model has been obtained, the remnant can be used to potentially improve precision. However, despite the “robustness” properties mentioned above, $\hat{y}^r(\cdot)$ must extrapolate reasonably well to the RCT, implying that the experimental sample cannot differ too substantially from the remnant. When $\hat{y}^r(\cdot)$ extrapolates poorly to the RCT, it is possible that remnant-based covariate adjustment can

actually harm precision. To make matters worse, the performance of $\hat{y}^r(\cdot)$ in the experimental sample—where it counts—may not be checked directly to select a best model, since outcomes from the RCT can not be touched when fitting $\hat{y}^r(\cdot)$. Thus, covariate adjustment using the remnant in this way is risky.

3.2 Flexibly Incorporating Remnant-Based Imputations

Consider a “generalized remnant estimator”

$$\hat{\tau}^{\text{GR}}(b) \equiv \frac{1}{n_t} \sum_{i \in \mathcal{T}} [Y_i - b\hat{y}^r(\mathbf{x}_i)] - \frac{1}{n_c} \sum_{i \in \mathcal{C}} [Y_i - b\hat{y}^r(\mathbf{x}_i)] \quad (13)$$

where b is some prespecified constant. Note that in the special case $b = 1$ this is the remnant estimator $\hat{\tau}^{\text{RE}}$, and in the special case $b = 0$ it is the simple difference-in-means $\hat{\tau}^{\text{DM}}$. Thus, following the discussion above, when $\hat{y}^r(\cdot)$ extrapolates well to the RCT, we wish to set $b = 1$, and when $\hat{y}^r(\cdot)$ extrapolates poorly to the RCT, we wish to set $b = 0$. More typically, an intermediate value for b may be optimal. The challenge is that we do not know *a priori* how well $\hat{y}^r(\cdot)$ extrapolates to the RCT, and therefore do not know the optimal choice for b .

There is good reason to suspect that sample splitting might be helpful in choosing b . In fact, the generalized remnant estimator can be formulated as a special case of the sample splitting estimator. First define $x^r \equiv \hat{y}^r(\mathbf{x})$. That is, we compute the remnant-based predictions of RCT outcomes as above (i.e., $\hat{y}^r(\mathbf{x})$), but now regard these predictions simply as a covariate to be used within the sample splitting estimator (i.e., x^r). Next consider the following imputation method, which is a constrained least squares (CLS) linear regression:

$$\hat{y}_{-i}^c(x_i^r) = a_{-i}^c + b_{-i}^c x_i^r \quad (14)$$

where

$$b_{-i}^c = b \quad (15)$$

$$a_{-i}^c = \arg \min_a \sum_{j \in \mathcal{C} \setminus i} [Y_j - (a + b x_j^r)]^2 \quad (16)$$

and where $\hat{y}_{-i}^t(x_i^r)$ is defined analogously. Here $\hat{y}_{-i}^c(\cdot)$ may be thought of as a univariate least squares linear regression of $Y_{\mathcal{C} \setminus i}$ on $x_{\mathcal{C} \setminus i}^r$ but where the slope coefficient b_{-i}^c is constrained to equal b . Denote the imputation strategy (14)–(16) as “CLS(b)”, and denote the resulting sample splitting estimator by $\hat{\tau}^{\text{SS}}[x^r; \text{CLS}(b)]$. Proposition 1 then follows.

Proposition 1.

$$\hat{\tau}^{\text{SS}}[x^r; \text{CLS}(b)] = \hat{\tau}^{\text{GR}}(b) \quad (17)$$

Proof. See Appendix A. □

Thus, in particular, $\hat{\tau}^{\text{SS}}[x^r; \text{CLS}(0)] = \hat{\tau}^{\text{DM}}$ and $\hat{\tau}^{\text{SS}}[x^r; \text{CLS}(1)] = \hat{\tau}^{\text{RE}}$. These observations suggest that, rather than prespecifying a value of b , we simply drop the constraint (15) and instead obtain both b_{-i}^c and a_{-i}^c by ordinary least squares, i.e., let

$$(a_{-i}^c, b_{-i}^c) = \arg \min_{(a,b)} \sum_{j \in \mathcal{C} \setminus i} [Y_j - (a + bx_j^r)]^2 \quad (18)$$

and similarly for (a_{-i}^t, b_{-i}^t) . We denote the resulting estimator $\hat{\tau}^{\text{SS}}[x^r, \text{LS}]$.

The estimator $\hat{\tau}^{\text{SS}}[x^r, \text{LS}]$ will typically be preferable to the remnant estimator $\hat{\tau}^{\text{RE}}$ because, for each observation i , the remaining $N - 1$ observations of the RCT help determine the best use of x_i^r in constructing \hat{m}_i . For example, suppose that the x^r are highly accurate imputations of the y^c in the RCT. In this case, we might expect $a_{-i}^c \approx 0$ and $b_{-i}^c \approx 1$ so that $\hat{y}_{-i}^c(x_i^r) \approx x_i^r$, or in other words, the remnant based predictions would “pass through” the linear regression largely unmodified, so that $\hat{\tau}^{\text{SS}}[x^r, \text{LS}] \approx \hat{\tau}^{\text{RE}}$. However, in contrast to the remnant estimator, poor imputations x^r will not necessarily harm precision in $\hat{\tau}^{\text{SS}}[x^r, \text{LS}]$. Consider the extreme case in which the x^r are pure noise. We would then expect $a_{-i}^c \approx \bar{Y}_{\mathcal{C} \setminus i}$ and $b_{-i}^c \approx 0$ so that $\hat{y}_{-i}^c(x_i^r) \approx \bar{Y}_{\mathcal{C} \setminus i}$. That is, we would revert approximately to mean-imputation, so that $\hat{\tau}^{\text{SS}}[x^r, \text{LS}] \approx \hat{\tau}^{\text{DM}}$. In other words, the role of x^r may be tempered according to the prediction accuracy of $\hat{y}^r(\cdot)$ in the RCT. We might therefore expect $\hat{\tau}^{\text{SS}}[x^r, \text{LS}]$ to nearly always outperform, or at least perform no worse than, $\hat{\tau}^{\text{RE}}$ and $\hat{\tau}^{\text{DM}}$. This intuition is formalized in the following proposition:

Proposition 2. *Let $(y_1^c, y_1^t, x_1^r), \dots, (y_N^c, y_N^t, x_N^r)$ be IID samples from a population in which y^c , y^t , and x^r have finite fourth moments, and where $-1 < \text{corr}(y^c, x^r) < 1$ and $-1 < \text{corr}(y^t, x^r) < 1$. Let b be a fixed constant. Let $\hat{\mathbb{V}}[\hat{\tau}^{\text{GR}}(b)]$ denote the estimated variance of $\hat{\tau}^{\text{GR}}(b)$, defined analogously to (4) and (12). Let $\hat{\mathbb{V}}\{\hat{\tau}^{\text{SS}}[x^r, \text{LS}]\}$ denote the estimated variance of $\hat{\tau}^{\text{SS}}[x^r, \text{LS}]$, defined as in (9). Then as $N \rightarrow \infty$,*

$$\frac{\hat{\mathbb{V}}\{\hat{\tau}^{\text{SS}}[x^r, \text{LS}]\}}{\hat{\mathbb{V}}[\hat{\tau}^{\text{GR}}(b)]} \xrightarrow{p} \phi(b) \leq 1$$

where $\phi(b)$ is some constant that depends on b .

Proof. See Appendix A. □

Notably, although this proposition is asymptotic in nature, we expect it to be relevant even in relatively small samples, given that $\hat{\tau}^{\text{SS}}[x^r, \text{LS}]$ effectively only requires estimating two more parameters than $\hat{\tau}^{\text{GR}}(b)$ (i.e., the slope coefficients b_{-i}^c and b_{-i}^t). Simulation studies in Appendix B appear to generally support this intuition; $\hat{\tau}^{\text{SS}}[x^r, \text{LS}]$ nearly always outperforms $\hat{\tau}^{\text{DM}}$, except in very small samples when the remnant-based predictions are poor, in which case $\hat{\tau}^{\text{SS}}[x^r, \text{LS}]$ performs only slightly worse than $\hat{\tau}^{\text{DM}}$. Indeed, in the ASSISTments experiments we analyze in Section 4 we see the greatest performance gains in the smallest RCT.

Importantly, because the x^r are used only as a covariate, they do not necessarily need to accurately impute the potential outcomes in the RCT; rather, it suffices that they are merely

predictive. If the RCT is systematically different from the remnant, e.g., the potential outcomes in the RCT differ in scale from those in the remnant, the x^r will still be useful as long as they are correlated with the experimental potential outcomes. Indeed, counterintuitively, it is even possible for $\hat{\tau}^{\text{SS}}[x^r, \text{LS}]$ to achieve precision gains if the x^r are *anticorrelated* with outcomes in the RCT.

3.3 Combining Remnant-Based and Within-RCT Covariate Adjustment

The estimator $\hat{\tau}^{\text{SS}}[x^r, \text{LS}]$ effectively solves the remnant estimator’s main deficiencies. However, $\hat{\tau}^{\text{SS}}[x^r, \text{LS}]$ largely neglects the RCT covariates, except to the extent that x^r depends on \mathbf{x} through $\hat{y}^r(\cdot)$. Neglecting the RCT covariate data may be suboptimal, especially when $\hat{y}^r(\cdot)$ is poorly predictive of outcomes in the RCT, perhaps due to systematic differences between the RCT and the remnant. Our goal in this section is to augment the strategy of the previous section, so that the RCT covariate data may be more fully exploited.

Define

$$\tilde{\mathbf{x}}_i \equiv (x_{i1}, x_{i2}, \dots, x_{ip}, x_i^r) \quad (19)$$

or in other words, $\tilde{\mathbf{x}}_i$ is \mathbf{x}_i augmented with x_i^r . We may now compute $\hat{\tau}^{\text{SS}}$ using the augmented set of covariates $\tilde{\mathbf{x}}$ instead of \mathbf{x} . The hope is that by including x^r we can exploit information in the remnant in much the same way that $\hat{\tau}^{\text{SS}}[x^r, \text{LS}]$ does, while simultaneously performing a more standard within-RCT covariate adjustment. For example, we might use random forests and compute $\hat{\tau}^{\text{SS}}[\tilde{\mathbf{x}}, \text{RF}]$.

In general, the precision of the estimator will depend on the performance of the imputation strategy, and in particular, its ability to integrate information from the remnant, via x^r , with information from other covariates \mathbf{x} . On the one hand, x^r is a function of the other covariates and thus, in at least some sense, does not contain any additional information. However, the function $\hat{y}^r(\cdot)$ is fitted on the remnant, which may be much larger than the experimental sample, and thus $\hat{y}^r(\cdot)$ may be a more accurate imputation function than what we would be able to obtain using the RCT data alone. In this sense, x^r does contain additional information, which can be exploited by the imputation method by heavily weighting x^r over the other covariates.

On the other hand, if the x^r are highly accurate, using them as a covariate within a nonlinear model like a random forest may be statistically inefficient compared to a linear model, as in $\hat{\tau}^{\text{SS}}[x^r, \text{LS}]$. Therefore, it may not always be clear whether a highly flexible method such as $\hat{\tau}^{\text{SS}}[\tilde{\mathbf{x}}, \text{RF}]$ will outperform $\hat{\tau}^{\text{SS}}[x^r, \text{LS}]$; it depends on the quality of the imputations x^r as well as the predictive power of the covariates in the experimental sample.

This suggests imputing potential outcomes using a specialized ensemble learner [e.g. Opitz and Maclin, 1999]: a weighted average of linear regression using just x_i^r , as in $\hat{\tau}^{\text{SS}}[x^r, \text{LS}]$, and random forests using $\tilde{\mathbf{x}}$, as in $\hat{\tau}^{\text{SS}}[\tilde{\mathbf{x}}, \text{RF}]$. More specifically, let $\hat{y}_{-i}^{c, \text{LS}}(\tilde{\mathbf{x}}_i)$ be the least squares imputation defined in (14) and (18), i.e., the imputation used within $\hat{\tau}^{\text{SS}}[x^r, \text{LS}]$; note in particular that $\hat{y}_{-i}^{c, \text{LS}}(\tilde{\mathbf{x}}_i)$ ignores all of the entries of $\tilde{\mathbf{x}}_i$ except x_i^r . Let $\hat{y}_{-i}^{c, \text{RF}}(\tilde{\mathbf{x}}_i)$ denote the imputation from a random forest regression of $Y_{C \setminus i}$ on $\tilde{\mathbf{x}}_{C \setminus i}$. We then define an ensemble

imputation

$$\hat{y}_{-i}^{c, \text{EN}}(\tilde{\mathbf{x}}_i) = \gamma_i^c \hat{y}_{-i}^{c, \text{LS}}(\tilde{\mathbf{x}}_i) + (1 - \gamma_i^c) \hat{y}_{-i}^{c, \text{RF}}(\tilde{\mathbf{x}}_i) \quad (20)$$

which is an interpolation between $\hat{y}_{-i}^{c, \text{LS}}(\tilde{\mathbf{x}}_i)$ and $\hat{y}_{-i}^{c, \text{RF}}(\tilde{\mathbf{x}}_i)$, where the interpolation parameter γ_i^c is such that $0 \leq \gamma_i^c \leq 1$ and is given by

$$\gamma_i^c = \arg \min_{\gamma \in [0, 1]} \sum_{j \in \mathcal{C} \setminus i} \left\{ Y_j - \left[\gamma \hat{y}_{-i, j}^{c, \text{LS}}(\tilde{\mathbf{x}}_j) + (1 - \gamma) \hat{y}_{-i, j}^{c, \text{RF}}(\tilde{\mathbf{x}}_j) \right] \right\}^2$$

where $\hat{y}_{-i, j}^{c, \text{LS}}(\tilde{\mathbf{x}}_j)$ is defined analogously to $\hat{y}_{-i}^{c, \text{LS}}(\tilde{\mathbf{x}}_i)$, but with both observations i and j removed, and similarly for $\hat{y}_{-i, j}^{c, \text{RF}}(\tilde{\mathbf{x}}_j)$. That is, the interpolation parameter γ_i^c is obtained empirically to minimize mean squared error, and is obtained from a leave-one-out procedure, which ensures that $\gamma_i^c \perp T_i$, and thus $\hat{y}_{-i}^{c, \text{EN}}(\tilde{\mathbf{x}}_i) \perp T_i$. We denote the resulting ensemble-based estimator $\hat{\tau}^{\text{SS}}[\tilde{\mathbf{x}}, \text{EN}]$. The imputation strategy (20) allows $\hat{\tau}^{\text{SS}}[\tilde{\mathbf{x}}, \text{EN}]$ to triangulate between $\hat{\tau}^{\text{SS}}[x^r, \text{LS}]$ and $\hat{\tau}^{\text{SS}}[\tilde{\mathbf{x}}, \text{RF}]$, and therefore combines the advantages of both, at the cost of estimating only one additional parameter (i.e., γ_i^c). We explore the performance of $\hat{\tau}^{\text{SS}}[\tilde{\mathbf{x}}, \text{EN}]$ in simulation studies in Appendix B, and find that $\hat{\tau}^{\text{SS}}[\tilde{\mathbf{x}}, \text{EN}]$ typically performs similarly to the better of $\hat{\tau}^{\text{SS}}[x^r, \text{LS}]$ or $\hat{\tau}^{\text{SS}}[\tilde{\mathbf{x}}, \text{RF}]$.

4 Estimating Effects in 33 Online Experiments

4.1 Data from the ASSISTments TestBed

We apply and evaluate the methods described in this work to a set of 33 randomized controlled experiments run within the ASSISTments TestBed, described in the Introduction. These A/B tests contrast a variety of pedagogical conditions in modules teaching 6th, 7th, and 8th grade mathematics content. For our purposes, the outcome of interest was completion of the module, a binary variable.

In general, once a TestBed proposal is approved, based on Institutional Review Board and content quality criteria, its experimental conditions are embedded into an ASSISTments assignment. This is then assigned to students, either by a group of teachers recruited by the researcher or, more commonly, by the existing population of teachers using ASSISTments in their classrooms. As an example, consider an experiment comparing text-based hints to video hints. The proposing researcher would create the alternative hints and embed them into particular assignable content, a “problem set.” Then, any time a teacher assigns that problem set to his or her students, those students are randomized to one of the conditions, and, when they request hints, receive them as either text or video.

There are several types of problem sets that researchers can utilize when developing their experiments. In the case of the 33 experiments observed in this work, the problem sets are mastery-based assignments called “skill builders.” As opposed to more traditional assignments requiring students to complete all problems assigned, skill builders require students to demonstrate a sufficient level of understanding in order to complete the assignment. By default, students must simply answer three consecutive problems correctly without the use

of computer-provided aid such as hints or scaffolding (a type of aid that breaks the problem into smaller steps). In this way, completion acts as a measure of knowledge and understanding as well as persistence and learning, as students will be continuously given more problems until they are able to reach the completion threshold. ASSISTments also includes a “daily limit” of ten problems to encourage students to seek help if they are struggling to reach the threshold.

After the completion of a TestBed experiment, the proposing researcher may download a dataset which includes students’ treatment assignments and their performance within the skill builder, including an indicator for completion. Additionally, the dataset includes aggregated features that describe student performance within the learning platform prior to random assignment for each respective experiment. Summary statistics for the nine covariates we used in our analyses, pooled across experiments, are displayed in Table 1. These include the numbers of problems worked, and assignments and homework assigned, percent of problems correct on first try, assignments completed, and homework completed at the student and class level, and students’ genders, as guessed by an internal ASSISTments algorithm based on first names. We imputed missing covariate values separately within each experiment. When possible, we used the mean of observed values from students in the same classroom; otherwise we used the grand mean. We combined this data with disaggregated log data from students’ individual prior assignments.

	Mean	SD	% Missing
Problem Count	603.11	784.29	2
Percent Correct	0.68	0.13	2
Assignments Assigned	103.92	412.15	13
Percent Completion	0.89	0.21	13
Class Percent Completion	0.90	0.13	22
Homework Assigned	25.82	29.87	50
Homework Percent Completion	0.93	0.16	59
Class Homework Percent Completion	0.93	0.09	56
Gussed Gender	Male: 36%	Female: 36%	Unknown: 28%

Table 1: Summary statistics for aggregate prior ASSISTments performance used as within-sample covariates: number of problems worked, and assignments and homework assigned, percent of problems correct on first try, assignments completed, and homework completed at the student and class level, and students’ genders, as guessed by ASSISTments based on first names.

4.2 Imputations from the Remnant

We also gathered analogous data from a large remnant of students who did not participate in any of the 33 experiments we analyzed. Ideally, the remnant would consist of previous ASSISTments students who had worked on the skill builders on which the 33 experiments had been run. If that were the case, we would have considered 33 outcomes of interest, say

Experiment	n		% Complete		Experiment	n		% Complete	
	Trt	Ctl	Trt	Ctl		Trt	Ctl	Trt	Ctl
1	956	961	93	93	18	188	193	89	85
2	330	365	98	96	19	199	213	89	82
3	680	650	86	88	20	264	281	81	79
4	943	921	70	68	21	242	266	81	76
5	931	900	61	64	22	215	211	82	82
6	355	349	88	88	23	281	234	73	69
7	492	463	79	81	24	269	288	65	59
8	231	197	92	91	25	224	233	73	74
9	367	387	83	82	26	270	253	63	61
10	617	587	67	62	27	228	244	68	64
11	338	289	88	84	28	201	228	73	69
12	478	476	76	73	29	238	259	44	54
13	193	209	93	89	30	74	92	91	84
14	404	451	73	69	31	69	67	91	87
15	265	275	85	84	32	76	81	62	70
16	165	170	92	89	33	15	11	73	55
17	259	246	82	85					

Table 2: Sample sizes and % homework completion—the outcome of interest—by treatment group in each of the 33 A/B tests.

Y_s , denoting completion of skill builder s . Unfortunately, due to labeling conventions in the ASSISTments database, this was only feasible for 11 of the 33 experiments. Instead, for all 33 experiments, we used prior ASSISTments data to impute one outcome, completion of a generic skill builder.

Rather than use the entire set of past ASSISTments users to build a remnant, we selected students who resembled those who participated in the 33 experiments. For the 11 experiments that we were able to match to other prior work, the remnant consisted of previous students who had worked at least one of the skill builders in the experiments. For the remaining 22 experiments, we first observed the collection of problem sets given to students in the experiments before being assigned. The remnant consisted of all other ASSISTments users who had been assigned to at least one of those assignments. In other words, the remnant consisted of students who did not participate in any of the 33 experiments, but had worked on some of the same content as those who did. In all, the remnant consisted of 175,528 students. Sample sizes and skill builder completion rates in the 33 experiments are given in Table 2.

We gathered records of up to ten assigned skill builders for each student in the remnant, and for each skill builder recorded the number of problems the student started, completed, requested help on, and answered correctly, the total amount of time spent, and assignment completion (i.e., skill mastery). Then, we fit a type of recurrent neural network [e.g. Williams

and Zipser, 1989] called Long-Short Term Memory (LSTM) [Hochreiter and Schmidhuber, 1997] to the resulting panel data. The model attempts to detect within-student trends in assignment completion and speed (i.e., the number of problems needed for skill mastery); please see Appendix C for further details. Using 10-fold cross validation within the remnant, we estimated the area under the ROC curve as 0.82 and a root mean squared error of 0.34 for the dependent measure of next assignment completion.

After fitting and validating the model in the remnant, we used it to predict skill builder completion for each subject in each of the 33 experiments. To do so, we gathered log data for each student from up to ten previous assigned skill builders. (Students in the experiments with no prior data were dropped from all analyses.) Using the model fit in the remnant, we predicted whether each student would complete his or her next assigned skill builder. The resulting predictive probabilities were used as x^r in the following analyses.

4.3 Results

In each of the 33 experiments, we calculated five different unbiased ATE estimates: [1] the simple difference-in-means estimator $\hat{\tau}^{\text{DM}}$ (equation 3); [2] the remnant estimator $\hat{\tau}^{\text{RE}}$ (equation 11); [3] $\hat{\tau}^{\text{SS}}[x^r, \text{LS}]$ (Section 3.2); [4] $\hat{\tau}^{\text{SS}}[\mathbf{x}; \text{RF}]$ (Section 2.3) where \mathbf{x} denotes only those covariates supplied within the TestBed, as listed in Table 1; and [5] $\hat{\tau}^{\text{SS}}[\tilde{\mathbf{x}}, \text{EN}]$ (Section 3.3), using both x^r and the provided TestBed covariates \mathbf{x} . These five methods are all design-based and unbiased, but they differ in their adjustment for covariates—both in the data they use for the adjustment, and in how the adjustment is effected. Notably, in this application the remnant-based predictions x^r are not functions only of \mathbf{x} . The covariates in \mathbf{x} are limited to aggregated data that summarize a student’s previous performance (Table 1), whereas the predictions x^r are based on a more fine-grained longitudinal analysis of each student’s log data.

Since each of these estimates is unbiased, we will focus on their estimated sampling variances. To aid interpretability, we will express contrasts between the sampling variances of two methods in terms of sample size. The estimated sampling variance of each estimator we consider is inversely proportional to sample size (see, e.g., equation 9). Therefore, reducing the sampling variance of an estimator by, say, 1/2 is equivalent to doubling its sample size. Under that reasoning, the following discussion will refer to the ratio of estimated sampling variances as a “sample size multiplier.”

4.3.1 Remnant-Based Adjustment: Comparing $\hat{\tau}^{\text{RE}}$ and $\hat{\tau}^{\text{SS}}[x^r, \text{LS}]$

Figure 1 compares $\hat{\tau}^{\text{DM}}$, $\hat{\tau}^{\text{RE}}$, and $\hat{\tau}^{\text{SS}}[x^r, \text{LS}]$ on the 33 ASSISTments TestBed experiments. Each dot in the figure corresponds to a sample size multiplier comparing two estimated sampling variances in a particular experiment. The vertical line at 1.0 indicates experiments in which the two methods gave approximately equal sampling variances. Dots to the right of the line correspond to experiments in which the variance in the denominator of the fraction was lower, and dots to the left of the line correspond to experiments in which the variance in the numerator was lower.

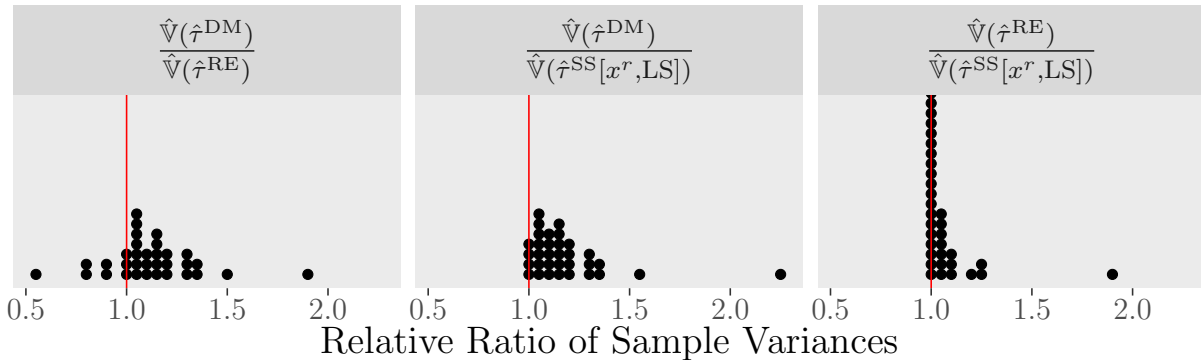


Figure 1: A dotplot showing sample size multipliers (i.e. sampling variance ratios) comparing $\hat{\tau}^{\text{DM}}$, $\hat{\tau}^{\text{RE}}$, and $\hat{\tau}^{\text{SS}}[x^r, \text{LS}]$ on the 33 ASSISTments TestBed experiments.

The leftmost plot contrasts $\hat{\tau}^{\text{RE}}$ with $\hat{\tau}^{\text{DM}}$. In three experiments, the variances of $\hat{\tau}^{\text{RE}}$ and $\hat{\tau}^{\text{DM}}$ were approximately equal, and in 25 experiments $\hat{\tau}^{\text{RE}}$ outperformed $\hat{\tau}^{\text{DM}}$. Notably, in one case (experiment #33) the adjustment provided by $\hat{\tau}^{\text{RE}}$ was equivalent to a roughly 90% increase in sample size, and in another (experiment #26) the adjustment was equivalent to a roughly 50% increase. On the other hand, in 5 experiments, the sampling variance of $\hat{\tau}^{\text{RE}}$ was higher than that of $\hat{\tau}^{\text{DM}}$. Most egregiously, in one experiment (#2) the adjustment given by $\hat{\tau}^{\text{RE}}$ was equivalent to a roughly 45% *decrease* in sample size. In this case, apparently, the imputations from the model fit to the remnant were particularly inaccurate in the experimental sample. Because experimental outcomes played no role whatsoever in determining the adjustment provided by $\hat{\tau}^{\text{RE}}$, the adjustment was blind to this inaccuracy, and was unable to anticipate the resulting increase in variance in those cases.

In contrast, the $\hat{\tau}^{\text{SS}}[x^r, \text{LS}]$ estimator incorporates information on imputation accuracy into its covariate adjustment. The middle panel of Figure 1 shows that across the board, $\hat{\tau}^{\text{SS}}[x^r, \text{LS}]$ variances were smaller or roughly equal to those of $\hat{\tau}^{\text{DM}}$. That is, $\hat{\tau}^{\text{SS}}[x^r, \text{LS}]$ successfully avoided the risk that poor imputations pose to $\hat{\tau}^{\text{RE}}$, and never increased variance relative to $\hat{\tau}^{\text{DM}}$. Moreover, in those cases in which $\hat{\tau}^{\text{RE}}$ performed well, $\hat{\tau}^{\text{SS}}[x^r, \text{LS}]$ tended to perform even better. For instance, in experiment #33, the adjustment provided by $\hat{\tau}^{\text{SS}}[x^r, \text{LS}]$ was equivalent to a roughly 130% increase in sample size (relative to $\hat{\tau}^{\text{DM}}$).

The rightmost panel of Figure 1 makes the comparison between $\hat{\tau}^{\text{RE}}$ and $\hat{\tau}^{\text{SS}}[x^r, \text{LS}]$ explicit: $\hat{\tau}^{\text{SS}}[x^r, \text{LS}]$ sample variances dominated those of $\hat{\tau}^{\text{RE}}$. In roughly half of the experiments, $\hat{\tau}^{\text{RE}}$ and $\hat{\tau}^{\text{SS}}[x^r, \text{LS}]$ performed similarly, and in the remaining half $\hat{\tau}^{\text{SS}}[x^r, \text{LS}]$ improved upon $\hat{\tau}^{\text{RE}}$. Proposition 2, above, guarantees that $\hat{\tau}^{\text{SS}}[x^r, \text{LS}]$ will dominate both $\hat{\tau}^{\text{DM}}$ and $\hat{\tau}^{\text{RE}}$ in the limit as $N \rightarrow \infty$; Figure 1 gives examples of this property in finite samples.

4.3.2 Incorporating Standard Covariates

Figure 2 compares $\hat{\tau}^{\text{SS}}[\tilde{x}, \text{EN}]$ to $\hat{\tau}^{\text{SS}}[x^r, \text{LS}]$, $\hat{\tau}^{\text{SS}}[\mathbf{x}; \text{RF}]$, and $\hat{\tau}^{\text{DM}}$, respectively, on the same 33 ASSISTments TestBed experiments. The left panel, comparing $\hat{\tau}^{\text{SS}}[x^r, \text{LS}]$ to $\hat{\tau}^{\text{SS}}[\tilde{x}, \text{EN}]$,

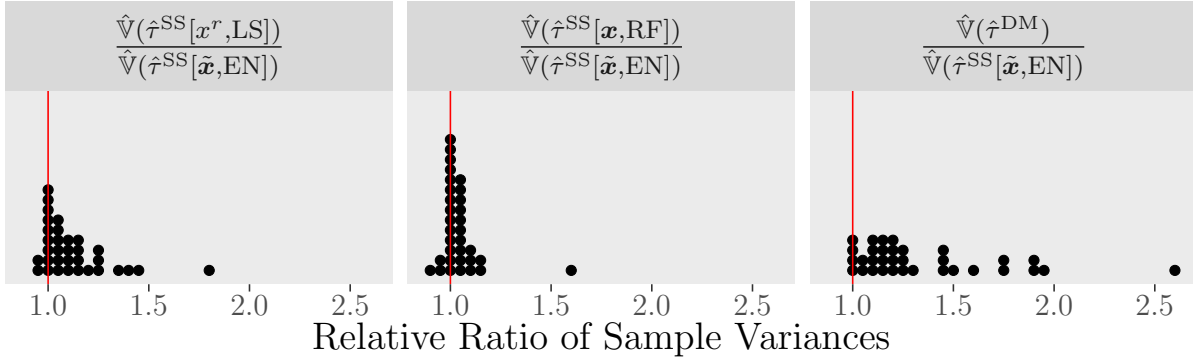


Figure 2: A dotplot showing sample size multipliers (i.e. sampling variance ratios) comparing $\hat{\tau}^{\text{SS}}[\tilde{\mathbf{x}}, \text{EN}]$ to $\hat{\tau}^{\text{SS}}[x^r, \text{LS}]$, $\hat{\tau}^{\text{SS}}[\mathbf{x}; \text{RF}]$, and $\hat{\tau}^{\text{DM}}$, respectively, on the 33 ASSISTments TestBed experiments.

shows the impact of including standard covariates, incorporating them as described in the ensemble approach of Section 3.3. In all but two cases, the sampling variance of $\hat{\tau}^{\text{SS}}[\tilde{\mathbf{x}}, \text{EN}]$ was less than or roughly equal to that of $\hat{\tau}^{\text{SS}}[x^r, \text{LS}]$ —that is, including standard covariates improved precision. In fifteen cases, this improvement was equivalent to increasing the sample size by more than 10%; in five of those cases the improvement was more than 25% and in one experiment, it was more than 80%.

The middle panel compares the sampling variances of $\hat{\tau}^{\text{SS}}[\tilde{\mathbf{x}}, \text{EN}]$ and $\hat{\tau}^{\text{SS}}[\mathbf{x}; \text{RF}]$, showing the extent to which including x^r improved precision relative to using only standard covariates. In all but three experiments the sampling variance of $\hat{\tau}^{\text{SS}}[\tilde{\mathbf{x}}, \text{EN}]$ was less than or roughly equal to the sampling variance of $\hat{\tau}^{\text{SS}}[\mathbf{x}; \text{RF}]$. In six experiments the improvement was equivalent to an increase in sample size of more than 10%, and in one of those cases, experiment #33, the improvement was equivalent to an almost 60% increase in sample size.

The rightmost panel compares the sampling variances of $\hat{\tau}^{\text{SS}}[\tilde{\mathbf{x}}, \text{EN}]$ and the simple difference-in-means estimator, showing the total impact of covariate adjustment on statistical precision. Across every one of the 33 experiments, the estimated sampling variances for $\hat{\tau}^{\text{SS}}[\tilde{\mathbf{x}}, \text{EN}]$ were lower or roughly equal to those of $\hat{\tau}^{\text{DM}}$. In 26 experiments the improvement was equivalent to increasing the sample size by more than 10%; in 15 of those the improvement was equivalent to a more than 25% increase in sample size, and in the case of experiment #33, the improvement was equivalent to a 160% increase in sample size.

5 Discussion

Randomized experiments and observational studies have complementary strengths. Randomized experiments allow for unbiased estimates with minimal statistical assumptions, but often suffer from small sample sizes. Observational studies, by contrast, may offer huge sample sizes, but typically suffer from confounding biases which must be adjusted for, often through statistical modeling with questionable assumptions. In this paper we have

attempted to combine the strengths of both. More specifically, we have sought to improve the precision of randomized experiments by exploiting the rich information available in a large observational dataset.

Our approach may be summarized as “first, do no harm.” A randomized experiment may be analyzed by taking a simple difference in means, which on its own provides a valid design-based unbiased estimate. The rationale for a more complicated analysis would be to improve precision. Our goal has therefore been to ensure that, in attempting to improve precision by incorporating observational data, we have not actually made matters worse. In particular, we have sought to ensure that (1) no biases in the observational data may “leak” into the analysis, (2) we can reasonably expect to improve precision, not harm it, and (3) inference may be justified by the experimental randomization, without the need for additional statistical modeling assumptions.

The results from the 33 A/B tests we analyzed suggest that incorporating information gleaned from the remnant of an experiment can indeed improve causal inference—but it does not always do so. The extent to which the remnant can help improve precision depends on the quality of the remnant-based predictions, and this in turn depends on both the quality of the remnant data and the algorithm $\hat{y}^r(\cdot)$. It is therefore important to include observational data judiciously—our methods dynamically adapt, taking advantage of observational data when it is useful and minimizing its role when it isn’t.

While we have focused on the ASSISTments platform in this paper, future work will explore what other sources of auxiliary data, and corresponding prediction algorithms, may be particularly well suited to improving the precision of RCTs typically encountered in education research. Indeed, one of the advantages of developing models on observational data in this manner is that a wide variety of models may be explored, tested, and iteratively improved upon before they are applied to an RCT.

References

- Peter M Aronow and Joel A Middleton. A class of unbiased estimators of the average treatment effect in randomized experiments. *Journal of Causal Inference*, 1(1):135–154, 2013.
- Peter M. Aronow, Donald P. Green, and Donald K. K. Lee. Sharp bounds on the variance in randomized experiments. *Ann. Statist.*, 42(3):850–871, 2014.
- Susan Athey, Raj Chetty, and Guido Imbens. Combining experimental and observational data to estimate treatment effects on long term outcomes. *arXiv preprint arXiv:2006.09676*, 2020.
- Heejung Bang and James M Robins. Doubly robust estimation in missing data and causal inference models. *Biometrics*, 61(4):962–973, 2005.
- Alexandre Belloni, Victor Chernozhukov, and Christian Hansen. Inference on treatment

- effects after selection among high-dimensional controls. *The Review of Economic Studies*, 81(2):608–650, 2014.
- Adam Bloniarz, Hanzhong Liu, Cun-Hui Zhang, Jasjeet S Sekhon, and Bin Yu. Lasso adjustments of treatment effect estimates in randomized experiments. *Proceedings of the National Academy of Sciences*, 113(27):7383–7390, 2016.
- Anthony F Botelho, Ryan S Baker, and Neil T Heffernan. Improving sensor-free affect detection using deep learning. In *International Conference on Artificial Intelligence in Education*, pages 40–51. Springer, 2017.
- F. J. Breidt, G. Claeskens, and J. D. Opsomer. Model-assisted estimation for complex surveys using penalised splines. *Biometrika*, 92(4):831–846, 12 2005.
- F Jay Breidt and Jean D Opsomer. Model-assisted survey estimation with modern prediction techniques. *Statistical Science*, 32(2):190–205, 2017.
- Leo Breiman. Random forests. *Machine learning*, 45(1):5–32, 2001.
- Rich Caruana. Multitask learning. *Machine learning*, 28(1):41–75, 1997.
- Victor Chernozhukov, Denis Chetverikov, Mert Demirer, Esther Duflo, Christian Hansen, Whitney Newey, and James Robins. Double/debiased machine learning for treatment and structural parameters. *The Econometrics Journal*, 21(1):C1–C68, 2018.
- Bénédicte Colnet, Imke Mayer, Guanhua Chen, Awa Dieng, Ruohong Li, Gaël Varoquaux, Jean-Philippe Vert, Julie Josse, and Shu Yang. Causal inference methods for combining randomized trials and observational studies: a review. *arXiv preprint arXiv:2011.08047*, 2020.
- Mehdi Dagdoug, Camelia Goga, and David Haziza. Model-assisted estimation through random forests in finite population sampling. *arXiv e-prints*, art. arXiv:2002.09736, February 2020.
- Irina Degtiar and Sherri Rose. A review of generalizability and transportability. *arXiv preprint arXiv:2102.11904*, 2021.
- Alex Deng, Ya Xu, Ron Kohavi, and Toby Walker. Improving the sensitivity of online controlled experiments by utilizing pre-experiment data. In *Proceedings of the sixth ACM international conference on Web search and data mining*, pages 123–132, 2013.
- Alexis Diamond and Jasjeet S Sekhon. Genetic matching for estimating causal effects: A general multivariate matching method for achieving balance in observational studies. *Review of Economics and Statistics*, 95(3):932–945, 2013.

- Wouter Duivesteijn, Tara Farzami, Thijs Putman, Evertjan Peer, Hilde JP Weerts, Jasper N Adegeest, Gerson Foks, and Mykola Pechenizkiy. Have it both ways—from a/b testing to a&b testing with exceptional model mining. In *Joint European Conference on Machine Learning and Knowledge Discovery in Databases*, pages 114–126. Springer, 2017.
- Andreea L Erciulescu, Nathan B Cruze, and Balgobin Nandram. Model-based county level crop estimates incorporating auxiliary sources of information. *Journal of the Royal Statistical Society: Series A (Statistics in Society)*, 182(1):283–303, 2019.
- Andreea L Erciulescu, Nathan B Cruze, and Balgobin Nandram. Statistical challenges in combining survey and auxiliary data to produce official statistics. *Journal of Official Statistics (JOS)*, 36(1), 2020.
- David A. Freedman. On regression adjustments to experimental data. *Advances in Applied Mathematics*, 40(2):180–193, 2008.
- Emily R Fyfe. Providing feedback on computer-based algebra homework in middle-school classrooms. *Computers in Human Behavior*, 63:568–574, 2016.
- Camelia Goga and Anne Ruiz-Gazen. Efficient estimation of non-linear finite population parameters by using non-parametrics. *Journal of the Royal Statistical Society: Series B: Statistical Methodology*, 76(1):113–140, 2014.
- Susan Gruber and Mark J van der Laan. A targeted maximum likelihood estimator of a causal effect on a bounded continuous outcome. *The International Journal of Biostatistics*, 6(1), 2010.
- George Gui. Combining observational and experimental data using first-stage covariates. *arXiv preprint arXiv:2010.05117*, 2020.
- Erin Hartman, Richard Grieve, Roland Ramsahai, and Jasjeet S Sekhon. From sample average treatment effect to population average treatment effect on the treated: combining experimental with observational studies to estimate population treatment effects. *Journal of the Royal Statistical Society Series A*, 10:1111, 2015.
- Neil T Heffernan and Cristina Lindquist Heffernan. The assistments ecosystem: building a platform that brings scientists and teachers together for minimally invasive research on human learning and teaching. *International Journal of Artificial Intelligence in Education*, 24(4):470–497, 2014.
- Sepp Hochreiter and Jürgen Schmidhuber. Long short-term memory. *Neural computation*, 9(8):1735–1780, 1997.
- Kurt Hornik, Maxwell Stinchcombe, and Halbert White. Multilayer feedforward networks are universal approximators. *Neural networks*, 2(5):359–366, 1989.

- Daniel G Horvitz and Donovan J Thompson. A generalization of sampling without replacement from a finite universe. *Journal of the American Statistical Association*, 47(260): 663–685, 1952.
- Maximilian Ilse, Patrick Forré, Max Welling, and Joris M Mooij. Efficient causal inference from combined observational and interventional data through causal reductions. *arXiv preprint arXiv:2103.04786*, 2021.
- Eloise E Kaizar. Incorporating both randomized and observational data into a single analysis. *Annual Review of Statistics and Its Application*, 2:49–72, 2015.
- Nathan Kallus, Aahlad Manas Puli, and Uri Shalit. Removing hidden confounding by experimental grounding. In S. Bengio, H. Wallach, H. Larochelle, K. Grauman, N. Cesa-Bianchi, and R. Garnett, editors, *Advances in Neural Information Processing Systems 31*, pages 10888–10897. Curran Associates, Inc., 2018.
- Diederik P Kingma and Jimmy Ba. Adam: A method for stochastic optimization. *arXiv preprint arXiv:1412.6980*, 2014.
- Kenneth R Koedinger and Elizabeth A McLaughlin. Closing the loop with quantitative cognitive task analysis. *International Educational Data Mining Society*, 2016.
- Sören R Künzel, Bradly C Stadie, Nikita Vemuri, Varsha Ramakrishnan, Jasjeet S Sekhon, and Pieter Abbeel. Transfer learning for estimating causal effects using neural networks. *arXiv preprint arXiv:1808.07804*, 2018.
- Jessica Lim, Rosalind Walley, Jiacheng Yuan, Jeen Liu, Abhishek Dabral, Nicky Best, Andrew Grieve, Lisa Hampson, Josephine Wolfram, Phil Woodward, Florence Yong, Xiang Zhang, and Ed Bowen. Minimizing patient burden through the use of historical subject-level data in innovative confirmatory clinical trials: review of methods and opportunities. *Therapeutic innovation & regulatory science*, 52(5):546–559, 2018.
- Kelly S McConville, Gretchen G Moisen, and Tracey S Frescino. A tutorial on model-assisted estimation with application to forest inventory. *Forests*, 11(2):244, 2020.
- Patrick McGuire, Shihfen Tu, Mary Ellin Logue, Craig A Mason, and Korinn Ostrow. Counterintuitive effects of online feedback in middle school math: Results from a randomized controlled trial in ASSISTments. *Educational Media International*, 54(3):231–244, 2017.
- Kelly L Moore and Mark J van der Laan. Covariate adjustment in randomized trials with binary outcomes: targeted maximum likelihood estimation. *Statistics in Medicine*, 28(1): 39–64, 2009.
- J. Neyman. On the application of probability theory to agricultural experiments. essay on principles. section 9. *Statistical Science*, 5:463–480, 1923. 1990; transl. by D.M. Dabrowska and T.P. Speed.

- David Opitz and Richard Maclin. Popular ensemble methods: An empirical study. *Journal of artificial intelligence research*, 11:169–198, 1999.
- Isaac M Opper. Improving average treatment effect estimates in small-scale randomized controlled trials. *EdWorkingPapers*, 2021. URL <https://edworkingpapers.org/sites/default/files/ai21-344.pdf>.
- Jean D Opsomer, F Jay Breidt, Gretchen G Moisen, and Göran Kauermann. Model-assisted estimation of forest resources with generalized additive models. *Journal of the American Statistical Association*, 102(478):400–409, 2007.
- Korinn S Ostrow, Doug Selent, Yan Wang, Eric G Van Inwegen, Neil T Heffernan, and Joseph Jay Williams. The assessment of learning infrastructure (ali): the theory, practice, and scalability of automated assessment. In *Proceedings of the Sixth International Conference on Learning Analytics & Knowledge*, pages 279–288. ACM, 2016.
- Alexander Peysakhovich and Akos Lada. Combining observational and experimental data to find heterogeneous treatment effects. *arXiv preprint arXiv:1611.02385*, 2016.
- Chris Piech, Jonathan Bassen, Jonathan Huang, Surya Ganguli, Mehran Sahami, Leonidas J Guibas, and Jascha Sohl-Dickstein. Deep knowledge tracing. In *Advances in Neural Information Processing Systems*, pages 505–513, 2015.
- Stuart J Pocock. The combination of randomized and historical controls in clinical trials. *Journal of chronic diseases*, 29(3):175–188, 1976.
- James M Robins. Robust estimation in sequentially ignorable missing data and causal inference models. In *Proceedings of the American Statistical Association*, volume 1999, pages 6–10. Indianapolis, IN, 2000.
- James M Robins, Andrea Rotnitzky, and Lue Ping Zhao. Estimation of regression coefficients when some regressors are not always observed. *Journal of the American statistical Association*, 89(427):846–866, 1994.
- Paul R. Rosenbaum. Covariance adjustment in randomized experiments and observational studies. *Statistical Science*, 17(3):286–327, 2002.
- Michael Rosenblum and Mark J Van Der Laan. Simple, efficient estimators of treatment effects in randomized trials using generalized linear models to leverage baseline variables. *The international journal of biostatistics*, 6(1), 2010.
- Evan Rosenman and Art B Owen. Designing experiments informed by observational studies. *arXiv preprint arXiv:2102.10237*, 2021.
- Evan Rosenman, Art B Owen, Michael Baiocchi, and Hailey Banack. Propensity score methods for merging observational and experimental datasets. *arXiv preprint arXiv:1804.07863*, 2018.

- Evan Rosenman, Guillaume Basse, Art Owen, and Michael Baiocchi. Combining observational and experimental datasets using shrinkage estimators. *arXiv preprint arXiv:2002.06708*, 2020.
- Dominik Rothenhäusler. Model selection for estimation of causal parameters. *arXiv preprint arXiv:2008.12892*, 2020.
- D.B. Rubin. Estimating causal effects of treatments in randomized and nonrandomized studies. *Journal of Educational Psychology; Journal of Educational Psychology*, 66(5):688, 1974.
- Piotr Rzepakowski and Szymon Jaroszewicz. Decision trees for uplift modeling with single and multiple treatments. *Knowledge and Information Systems*, 32(2):303–327, 2012.
- Adam C Sales, Anthony Botelho, Thanaporn M Patikorn, and Neil T Heffernan. Using big data to sharpen design-based inference in a/b tests. In *Proceedings of the 11th International Conference on Educational Data Mining. International Educational Data Mining Society*, pages 479–486, 2018a.
- Adam C Sales, Ben B Hansen, and Brian Rowan. Rebar: Reinforcing a matching estimator with predictions from high-dimensional covariates. *Journal of Educational and Behavioral Statistics*, 43(1):3–31, 2018b.
- Carl-Erik Särndal, Bengt Swensson, and Jan Wretman. *Model assisted survey sampling*. Springer Science & Business Media, 2003.
- Anton Maximilian Schäfer and Hans Georg Zimmermann. Recurrent neural networks are universal approximators. In *International Conference on Artificial Neural Networks*, pages 632–640. Springer, 2006.
- Daniel O. Scharfstein, Andrea Rotnitzky, and James M. Robins. Rejoinder. *Journal of the American Statistical Association*, 94(448):1135–1146, 1999.
- Peter Z Schochet. Statistical theory for the RCT-YES software: Design-based causal inference for RCTs. NCEE 2015-4011. *National Center for Education Evaluation and Regional Assistance*, 2015.
- George AF Seber and Alan J Lee. *Linear regression analysis*, volume 329. John Wiley & Sons, 2012.
- Douglas Selent, Thanaporn Patikorn, and Neil Heffernan. Assistments dataset from multiple randomized controlled experiments. In *Proceedings of the Third (2016) ACM Conference on Learning@ Scale*, pages 181–184. ACM, 2016.
- Jon Arni Steingrímsson, Daniel F Hanley, and Michael Rosenblum. Improving precision by adjusting for prognostic baseline variables in randomized trials with binary outcomes, without regression model assumptions. *Contemporary clinical trials*, 54:18–24, 2017.

- R. Tibshirani. Regression shrinkage and selection via the lasso. *Journal of the Royal Statistical Society. Series B (Methodological)*, pages 267–288, 1996.
- Anastasios A Tsiatis, Marie Davidian, Min Zhang, and Xiaomin Lu. Covariate adjustment for two-sample treatment comparisons in randomized clinical trials: a principled yet flexible approach. *Statistics in medicine*, 27(23):4658–4677, 2008.
- Mark J Van der Laan and Sherri Rose. *Targeted learning: causal inference for observational and experimental data*. Springer Science & Business Media, 2011.
- Mark J van der Laan and Daniel Rubin. Targeted maximum likelihood learning. *The International Journal of Biostatistics*, 2(1), 2006.
- Pablo E Verde and Christian Ohmann. Combining randomized and non-randomized evidence in clinical research: a review of methods and applications. *Research synthesis methods*, 6(1):45–62, 2015.
- Kert Viele, Scott Berry, Beat Neuenschwander, Billy Amzal, Fang Chen, Nathan Enas, Brian Hobbs, Joseph G Ibrahim, Nelson Kinnersley, Stacy Lindborg, et al. Use of historical control data for assessing treatment effects in clinical trials. *Pharmaceutical statistics*, 13(1):41–54, 2014.
- Stefan Wager, Wenfei Du, Jonathan Taylor, and Robert J Tibshirani. High-dimensional regression adjustments in randomized experiments. *Proceedings of the National Academy of Sciences*, 113(45):12673–12678, 2016.
- Candace Walkington, Virginia Clinton, and Anthony Sparks. The effect of language modification of mathematics story problems on problem-solving in online homework. *Instructional Science*, pages 1–31, 2019.
- Li Wang and Suojin Wang. Nonparametric additive model-assisted estimation for survey data. *Journal of Multivariate Analysis*, 102(7):1126–1140, 2011.
- P. J. Werbos. Backpropagation through time: what it does and how to do it. *Proceedings of the IEEE*, 78(10):1550–1560, 1990.
- Ronald J Williams and David Zipser. A learning algorithm for continually running fully recurrent neural networks. *Neural computation*, 1(2):270–280, 1989.
- Edward Wu and Johann A. Gagnon-Bartsch. The LOOP estimator: Adjusting for covariates in randomized experiments. *Evaluation Review*, 42(4):458–488, 2018.
- Edward Wu and Johann A. Gagnon-Bartsch. Design-based covariate adjustments in paired experiments. *Journal of Educational and Behavioral Statistics*, 46(1):109–132, 2021.
- Jiacheng Yuan, Jeen Liu, Ray Zhu, Ying Lu, and Ulo Palm. Design of randomized controlled confirmatory trials using historical control data to augment sample size for concurrent controls. *Journal of Biopharmaceutical Statistics*, 29(3):558–573, 2019.

Siyuan Zhao and Neil Heffernan. Estimating individual treatment effect from educational studies with residual counterfactual networks. In *Proceedings of the 10th International Conference on Educational Data Mining, EDM*, 2017.

DRAFT

A Propositions

Proposition 1.

$$\hat{\tau}^{\text{SS}}[x^r; \text{CLS}(b)] = \hat{\tau}^{\text{GR}}(b) \quad (17)$$

Proof. First note that

$$\begin{aligned} a_{-i}^c &= \arg \min_a \sum_{j \in \mathcal{C} \setminus i} [(Y_j - bx_j^r) - a]^2 \\ &= \frac{1}{n_c - (1 - T_i)} \sum_{j \in \mathcal{C} \setminus i} (Y_j - bx_j^r) \end{aligned}$$

and similarly

$$a_{-i}^t = \frac{1}{n_t - T_i} \sum_{j \in \mathcal{T} \setminus i} (Y_j - bx_j^r)$$

and therefore

$$\hat{m}_i = \begin{cases} \frac{(1-p) \sum_{j \in \mathcal{T}} (Y_j - bx_j^r)}{n_t} + \frac{p \sum_{j \in \mathcal{C} \setminus i} (Y_j - bx_j^r)}{n_c - 1} + bx_i^r & T_i = 0 \\ \frac{(1-p) \sum_{j \in \mathcal{T} \setminus i} (Y_j - bx_j^r)}{n_t - 1} + \frac{p \sum_{j \in \mathcal{C}} (Y_j - bx_j^r)}{n_c} + bx_i^r & T_i = 1. \end{cases}$$

Thus, $\hat{\tau}^{\text{SS}}[x^r; \text{CLS}(b)]$ (abbreviated $\hat{\tau}^{\text{SS}}$ below) is given by

$$\begin{aligned} \hat{\tau}^{\text{SS}} &= \frac{1}{N} \left[\sum_{i \in \mathcal{T}} \frac{1}{p} (Y_i - \hat{m}_i) + \sum_{i \in \mathcal{C}} \frac{-1}{1-p} (Y_i - \hat{m}_i) \right] \\ &= \frac{1}{N} \left\{ \sum_{i \in \mathcal{T}} \frac{1}{p} \left[Y_i - \left(\frac{(1-p) \sum_{j \in \mathcal{T} \setminus i} (Y_j - bx_j^r)}{n_t - 1} + \frac{p \sum_{j \in \mathcal{C}} (Y_j - bx_j^r)}{n_c} + bx_i^r \right) \right] + \right. \\ &\quad \left. \sum_{i \in \mathcal{C}} \frac{-1}{1-p} \left[Y_i - \left(\frac{(1-p) \sum_{j \in \mathcal{T}} (Y_j - bx_j^r)}{n_t} + \frac{p \sum_{j \in \mathcal{C} \setminus i} (Y_j - bx_j^r)}{n_c - 1} + bx_i^r \right) \right] \right\} \\ &= \frac{1}{N} \left\{ \sum_{i \in \mathcal{T}} \frac{1}{p} \left[(Y_i - bx_i^r) - \left(\frac{(1-p) \sum_{j \in \mathcal{T} \setminus i} (Y_j - bx_j^r)}{n_t - 1} + \frac{p \sum_{j \in \mathcal{C}} (Y_j - bx_j^r)}{n_c} \right) \right] + \right. \\ &\quad \left. \sum_{i \in \mathcal{C}} \frac{-1}{1-p} \left[(Y_i - bx_i^r) - \left(\frac{(1-p) \sum_{j \in \mathcal{T}} (Y_j - bx_j^r)}{n_t} + \frac{p \sum_{j \in \mathcal{C} \setminus i} (Y_j - bx_j^r)}{n_c - 1} \right) \right] \right\}. \end{aligned}$$

If we now define $Z_i = Y_i - bx_i^r$, then

$$\begin{aligned} \hat{\tau}^{\text{SS}} &= \frac{1}{N} \left\{ \sum_{i \in \mathcal{T}} \frac{1}{p} \left[Z_i - \left(\frac{(1-p) \sum_{j \in \mathcal{T} \setminus i} Z_j}{n_t - 1} + \frac{p \sum_{j \in \mathcal{C}} Z_j}{n_c} \right) \right] + \right. \\ &\quad \left. \sum_{i \in \mathcal{C}} \frac{-1}{1-p} \left[Z_i - \left(\frac{(1-p) \sum_{j \in \mathcal{T}} Z_j}{n_t} + \frac{p \sum_{j \in \mathcal{C} \setminus i} Z_j}{n_c - 1} \right) \right] \right\} \end{aligned}$$

$$\begin{aligned}
&= \frac{1}{N} \left[\sum_{i \in \mathcal{T}} \left(\frac{Z_i}{p} - \frac{1-p}{p} \frac{\sum_{j \in \mathcal{T} \setminus i} Z_j}{n_t - 1} - \frac{\sum_{j \in \mathcal{C}} Z_j}{n_c} \right) + \right. \\
&\quad \left. \sum_{i \in \mathcal{C}} \left(-\frac{Z_i}{1-p} + \frac{\sum_{j \in \mathcal{T}} Z_j}{n_t} + \frac{p}{1-p} \frac{\sum_{j \in \mathcal{C} \setminus i} Z_j}{n_c - 1} \right) \right] \\
&= \frac{1}{N} \left[\sum_{i \in \mathcal{T}} \frac{Z_i}{p} - \sum_{i \in \mathcal{C}} \frac{Z_i}{1-p} - \frac{1-p}{p} \frac{(n_t - 1) \sum_{j \in \mathcal{T}} Z_j}{n_t - 1} - \frac{n_t \sum_{j \in \mathcal{C}} Z_j}{n_c} + \right. \\
&\quad \left. \frac{n_c \sum_{j \in \mathcal{T}} Z_j}{n_t} + \frac{p}{1-p} \frac{(n_c - 1) \sum_{j \in \mathcal{C}} Z_j}{n_c - 1} \right] \\
&= \frac{1}{N} \left[\sum_{i \in \mathcal{T}} \frac{Z_i - (1-p)Z_i}{p} - \sum_{i \in \mathcal{C}} \frac{Z_i - pZ_i}{1-p} - \frac{n_t \sum_{j \in \mathcal{C}} Z_j}{n_c} + \frac{n_c \sum_{j \in \mathcal{T}} Z_j}{n_t} \right] \\
&= \frac{1}{N} \left[\sum_{i \in \mathcal{T}} Z_i - \sum_{i \in \mathcal{C}} Z_i - \frac{n_t \sum_{j \in \mathcal{C}} Z_j}{n_c} + \frac{n_c \sum_{j \in \mathcal{T}} Z_j}{n_t} \right] \\
&= \frac{1}{N} \left[\frac{(n_c + n_t) \sum_{j \in \mathcal{T}} Z_j}{n_t} - \frac{(n_t + n_c) \sum_{j \in \mathcal{C}} Z_j}{n_c} \right] \\
&= \frac{\sum_{j \in \mathcal{T}} Z_j}{n_t} - \frac{\sum_{j \in \mathcal{C}} Z_j}{n_c}
\end{aligned}$$

which is the same as (13). \square

Proposition 2. Let $(y_1^c, y_1^t, x_1^r), \dots, (y_N^c, y_N^t, x_N^r)$ be IID samples from a population in which y^c , y^t , and x^r have finite fourth moments, and where $-1 < \text{corr}(y^c, x^r) < 1$ and $-1 < \text{corr}(y^t, x^r) < 1$. Let b be a fixed constant. Let $\hat{\mathbb{V}}[\hat{\tau}^{\text{GR}}(b)]$ denote the estimated variance of $\hat{\tau}^{\text{GR}}(b)$, defined analogously to (4) and (12). Let $\hat{\mathbb{V}}\{\hat{\tau}^{\text{SS}}[x^r, \text{LS}]\}$ denote the estimated variance of $\hat{\tau}^{\text{SS}}[x^r, \text{LS}]$, defined as in (9). Then as $N \rightarrow \infty$,

$$\frac{\hat{\mathbb{V}}\{\hat{\tau}^{\text{SS}}[x^r, \text{LS}]\}}{\hat{\mathbb{V}}[\hat{\tau}^{\text{GR}}(b)]} \xrightarrow{p} \phi(b) \leq 1$$

where $\phi(b)$ is some constant that depends on b .

Proof. We first explicitly define $\hat{\mathbb{V}}[\hat{\tau}^{\text{GR}}(b)]$. Let $R_i^{\text{GR}} = Y_i - bx_i^r$ and define

$$\hat{\mathbb{V}}[\hat{\tau}^{\text{GR}}(b)] = \frac{S^2(R_{\mathcal{C}}^{\text{GR}})}{n_c} + \frac{S^2(R_{\mathcal{T}}^{\text{GR}})}{n_t}. \quad (21)$$

Comparing (21) to (10) we see that in order to prove the desired result, it is sufficient to show that $\hat{E}_c^2/S^2(R_{\mathcal{C}}^{\text{GR}}) \xrightarrow{p} \phi_c(b) \leq 1$ and $\hat{E}_t^2/S^2(R_{\mathcal{T}}^{\text{GR}}) \xrightarrow{p} \phi_t(b) \leq 1$ where $\phi_c(b)$ and $\phi_t(b)$ are constants that depend on b . We will show $\hat{E}_c^2/S^2(R_{\mathcal{C}}^{\text{GR}}) \xrightarrow{p} \phi_c(b) \leq 1$; the argument for $\hat{E}_t^2/S^2(R_{\mathcal{T}}^{\text{GR}}) \xrightarrow{p} \phi_t(b) \leq 1$ is analogous.

Let \tilde{E}_c^2 be defined similarly to \hat{E}_c^2 , except that \tilde{E}_c^2 does not use leave-one-out predictions, and instead uses predictions based on all of the data. That is,

$$\tilde{E}_c^2 = \frac{1}{n_c} \sum_{i \in \mathcal{C}} [\tilde{y}^c(x_i^r) - y_i^c]^2 \quad (22)$$

where $\tilde{y}^c(x_i^r) = \tilde{a}^c + \tilde{b}^c x_i^r$ and where \tilde{a}^c and \tilde{b}^c are the intercept and slope coefficients, respectively, from a univariate regression of $Y_{\mathcal{C}}$ on $x_{\mathcal{C}}^r$ (not dropping observation i). Now note the following: (a) both $S^2(R_{\mathcal{C}}^{\text{GR}})$ and \tilde{E}_c^2 converge to finite constants; (b) the constant to which $S^2(R_{\mathcal{C}}^{\text{GR}})$ converges is not 0; and (c) $\tilde{E}_c^2 \leq S^2(R_{\mathcal{C}}^{\text{GR}})$ for all $n_c \geq 2$. (a) is ensured by the moment conditions. (b) is ensured by the condition $-1 < \text{corr}(y^c, x^r) < 1$. (c) follows from the fact that $\tilde{E}_c^2 = \frac{1}{n_c} \min_{(a,b)} \sum_{j \in \mathcal{C} \setminus i} [Y_j - (a + bx_j^r)]^2$ whereas $S^2(R_{\mathcal{C}}^{\text{GR}}) = \frac{1}{n_c - 1} \min_a \sum_{j \in \mathcal{C} \setminus i} [Y_j - (a + bx_j^r)]^2$ for a fixed value of b , and thus the minimization problem of the former is less constrained than the latter. As a result of (a), (b), and (c), it follows that $\tilde{E}_c^2 / S^2(R_{\mathcal{C}}^{\text{GR}}) \xrightarrow{p} \tilde{\phi}_c(b) \leq 1$.

To complete the proof, it suffices to show that $\hat{E}_c^2 \xrightarrow{p} \tilde{E}_c^2$. After some algebra,

$$\hat{E}_c^2 = \frac{1}{n_c} \sum_{i \in \mathcal{C}} [\tilde{y}^c(x_i^r) - y_i^c]^2 / (1 - h_i)^2 \quad (23)$$

where

$$h_i = \frac{1}{(n_c - 1)S^2(x_{\mathcal{C}}^r)} \left[\overline{(x_{\mathcal{C}}^r)^2} - 2\overline{x_{\mathcal{C}}^r}x_i^r + (x_i^r)^2 \right]. \quad (24)$$

Here, the h_i are the diagonal entries of the hat matrix from the regression of $Y_{\mathcal{C}}$ on $x_{\mathcal{C}}^r$ and we use the well-known shortcut formula for calculating leave-one-out residuals [Seber and Lee, 2012]. Note that $0 < h_i \leq 1$. Thus,

$$|\hat{E}_c^2 - \tilde{E}_c^2| \leq \left[\frac{1}{(1 - h^*)^2} - 1 \right] \tilde{E}_c^2 \quad (25)$$

where $h^* = \max_{\mathcal{C}} h_i$. However, because of the moment conditions on x^r , it is straightforward to show that $h^* \xrightarrow{p} 0$, and therefore $\hat{E}_c^2 \xrightarrow{p} \tilde{E}_c^2$. \square

B Simulations

We examine the performance of the estimators using simulations. In particular, we investigate the effects of varying sample size, the predictive power of the within-experiment covariates \mathbf{x} , and the predictive power of the remnant-based predictions x^r . We generate our data using a model that is parameterized in such a way that we are able to independently vary these three quantities (sample size, the predictive power of the covariates, and the predictive power of the remnant predictions).

We simulate a randomized experiment in which there are N subjects. For each subject i there are two covariates, $x_{i,1}$ and $x_{i,2}$, which are independent and $\text{Unif}(0, 10)$. The potential outcomes are generated from the following linear model:

$$\begin{aligned} a_i &= 2x_{i,1} + x_{i,2} + \delta_i \\ y_i^c &= \frac{a_i}{\sigma_a} \\ y_i^t &= y_i^c + 3 \end{aligned}$$

where $\delta_i \sim \text{N}(0, \sigma^2)$ and $\sigma_a^2 \equiv \text{Var}(a_i) = \frac{500}{12} + \sigma^2$. By generating our potential outcomes as above, we have defined our generative model so that the potential outcomes have unit variance. We can alternatively write the observed outcome as:

$$Y_i = 3T_i + \frac{2}{\sigma_a}x_{i,1} + \frac{1}{\sigma_a}x_{i,2} + \epsilon_i$$

where $\epsilon_i \sim \text{N}(0, \sigma^2/\sigma_a^2)$.

For each observation, we also simulate remnant predictions x_i^r by taking the true y_i^c and adding a normally distributed noise term with mean 0 and variance σ_{rem}^2 .

Again, our goal is to investigate variations in sample size, the predictive power of the covariates, and the predictive power of the remnant predictions. Sample size is directly indexed by N . We index the predictive power of the covariates with

$$R_{cov}^2 = 1 - \frac{\sigma^2}{\sigma_a^2}.$$

Similarly, the predictive power of the remnant prediction x_i^r is

$$R_{rem}^2 = 1 - \frac{\sigma_{rem}^2}{\text{Var}(x_i^r)} = 1 - \frac{\sigma_{rem}^2}{1 + \sigma_{rem}^2}.$$

Thus, given a desired R_{cov}^2 and R_{rem}^2 , the corresponding values of σ^2 and σ_{rem}^2 are:

$$\begin{aligned} \sigma^2 &= \frac{1 - R_{cov}^2}{R_{cov}^2} \times \frac{500}{12} \\ \sigma_{rem}^2 &= \frac{1 - R_{rem}^2}{R_{rem}^2}. \end{aligned}$$

We perform three sets of simulations. In each, we vary one of the quantities N , R_{cov}^2 , or R_{rem}^2 while holding the other two fixed. For each set of simulations, we compare the following methods:

1. $\hat{\tau}^{DM}$ – Simple difference-in-means estimator
2. $\hat{\tau}^{SS}[\mathbf{x}; \text{RF}]$ – RCT covariates only (Section 2.3)
3. $\hat{\tau}^{SS}[x^r, \text{LS}]$ – remnant-based predictions only (Section 3.2)
4. $\hat{\tau}^{SS}[\tilde{\mathbf{x}}, \text{RF}]$ – RCT covariates and remnant-based predictions (Section 3.3)
5. $\hat{\tau}^{SS}[\tilde{\mathbf{x}}, \text{EN}]$ – RCT covariates and remnant-based predictions (Section 3.3)

We use the following simulation procedure: For a given set of N , R_{cov}^2 , and R_{rem}^2 , we perform $k = 1000$ trials. For each trial, we generate a set of covariates, potential outcomes, a treatment assignment vector, and remnant predictions as described above. We then produce an estimate of the variance of each of the five methods. Next, we average the estimated variance across the k trials. Finally, we plot the average variance for each of the adjustment methods relative to the variance of $\hat{\tau}^{DM}$. That is, for each method (1) – (5) we plot (average variance of method) / (average variance of simple difference estimator).

Varying Sample Size For these simulations, we hold the predictive power of the covariates and remnant predictions constant and vary the sample size. We consider four scenarios: (1) $R_{rem}^2 = 0.25, R_{cov}^2 = 0.25$; (2) $R_{rem}^2 = 0.75, R_{cov}^2 = 0.25$; (3) $R_{rem}^2 = 0.25, R_{cov}^2 = 0.75$; and (4) $R_{rem}^2 = 0.75, R_{cov}^2 = 0.75$. In each scenario the sample sizes considered are $N = 30, 40, 50, 75, 100, 150, 200$. Results are in Figure 3.

All methods perform better than the simple difference estimator (the relative variances are all less than 1, with only a few exceptions), suggesting that adjustment is typically helpful. Both $\hat{\tau}^{SS}[\tilde{\mathbf{x}}, \text{RF}]$ and $\hat{\tau}^{SS}[\tilde{\mathbf{x}}, \text{EN}]$ typically outperform $\hat{\tau}^{SS}[\mathbf{x}; \text{RF}]$, indicating that incorporating the remnant predictions is typically beneficial. The exception is when the covariates are highly informative but the remnant predictions are not ($R_{rem}^2 = 0.25, R_{cov}^2 = 0.75$, lower left panel) and the sample size is small, in which case $\hat{\tau}^{SS}[\tilde{\mathbf{x}}, \text{RF}]$ performs slightly worse than $\hat{\tau}^{SS}[\mathbf{x}; \text{RF}]$.

We also observe that $\hat{\tau}^{SS}[\tilde{\mathbf{x}}, \text{EN}]$ does well at tracking its better performing component ($\hat{\tau}^{SS}[x^r, \text{LS}]$ or $\hat{\tau}^{SS}[\tilde{\mathbf{x}}, \text{RF}]$). It performs reasonably well at small sample sizes, and quickly converges to near optimal at larger sample sizes. In some cases $\hat{\tau}^{SS}[\tilde{\mathbf{x}}, \text{EN}]$ performs better than either component individually.

Varying Predictive Power of Remnant Prediction In these simulations, we hold the predictive power of the covariates and sample size constant and vary R_{rem}^2 . We again consider four scenarios, with N fixed at either 30 or 60, and R_{cov}^2 fixed at either 0.25 or 0.75. The values of R_{rem}^2 considered are $R_{rem}^2 = 0.05, 0.15, \dots, 0.85, 0.95$. Results are in Figure 4.

Once again, we observe that $\hat{\tau}^{SS}[\tilde{\mathbf{x}}, \text{EN}]$ tends to perform at least as well as either of its two components. This is particularly true for $N = 60$, where $\hat{\tau}^{SS}[\tilde{\mathbf{x}}, \text{EN}]$ closely follows

(or drops below) the lower of the component lines. As expected, the three methods that incorporate the remnant predictions all improve as R_{rem}^2 increases, while the performance of $\hat{\tau}^{SS}[\mathbf{x}; \text{RF}]$ stays constant. We see that $\hat{\tau}^{SS}[\tilde{\mathbf{x}}, \text{EN}]$ is notably outperformed by $\hat{\tau}^{SS}[\mathbf{x}; \text{RF}]$ only when R_{rem}^2 is lower than R_{cov}^2 and the sample size is small.

Varying Predictive Power of Covariates For this simulation, we hold the predictive power of the remnant predictions and sample size constant and vary $R_{cov}^2 = 0.05, 0.15, \dots, 0.85, 0.95$. We consider four scenarios: (1) $N = 30, R_{rem}^2 = 0.25$; (2) $N = 30, R_{rem}^2 = 0.75$; (3) $N = 60, R_{rem}^2 = 0.25$; and (4) $N = 60, R_{rem}^2 = 0.75$. Results are in Figure 5.

Here the performance of $\hat{\tau}^{SS}[x^r, \text{LS}]$ stays constant, as it makes use only of the remnant predictions, not the covariates. The remaining methods all improve as R_{cov}^2 increases. As before, we can see that $\hat{\tau}^{SS}[\tilde{\mathbf{x}}, \text{EN}]$ tracks its better performing component reasonably well, especially when $N = 60$.

DRAFT

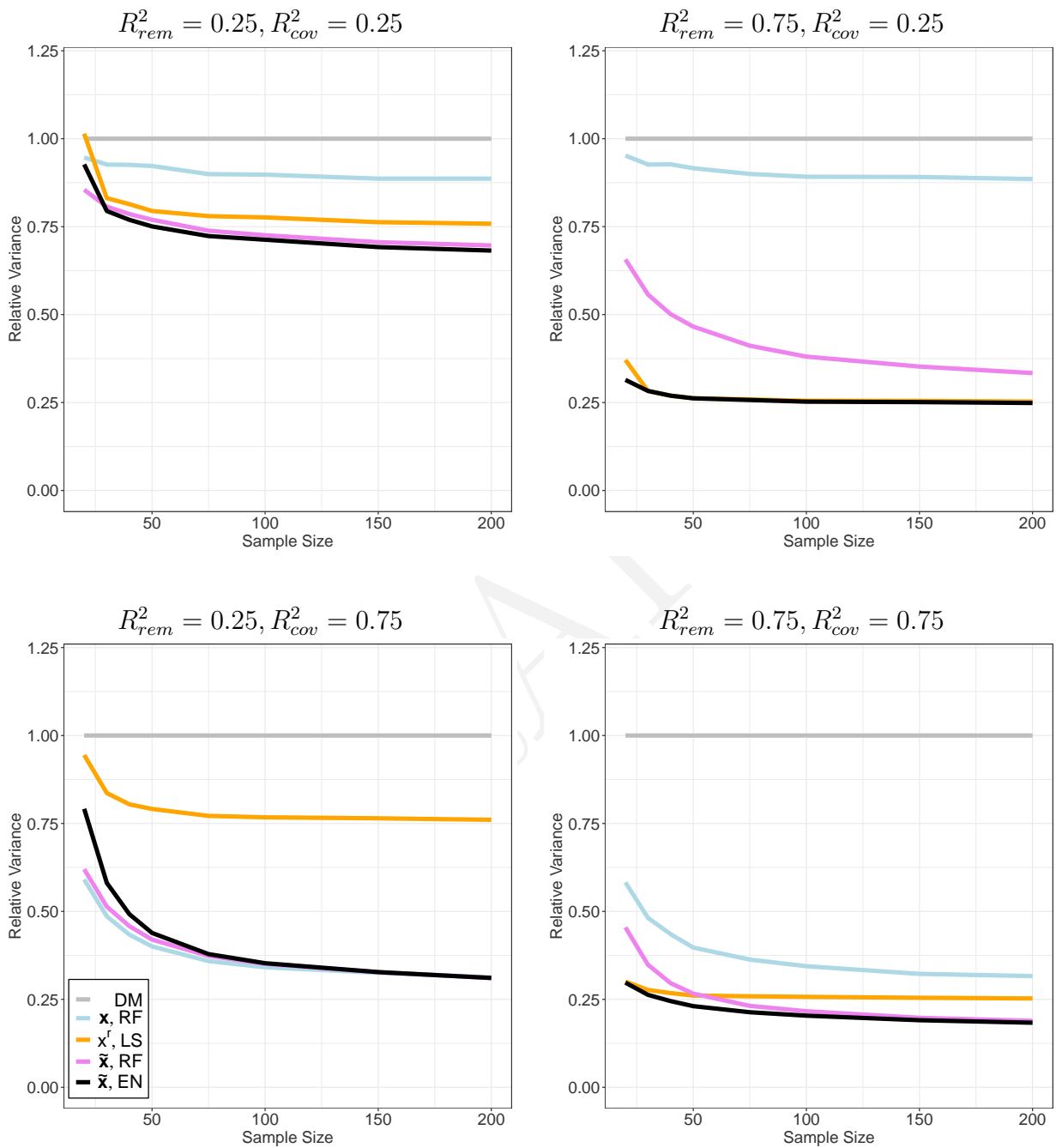


Figure 3: Varying sample size.

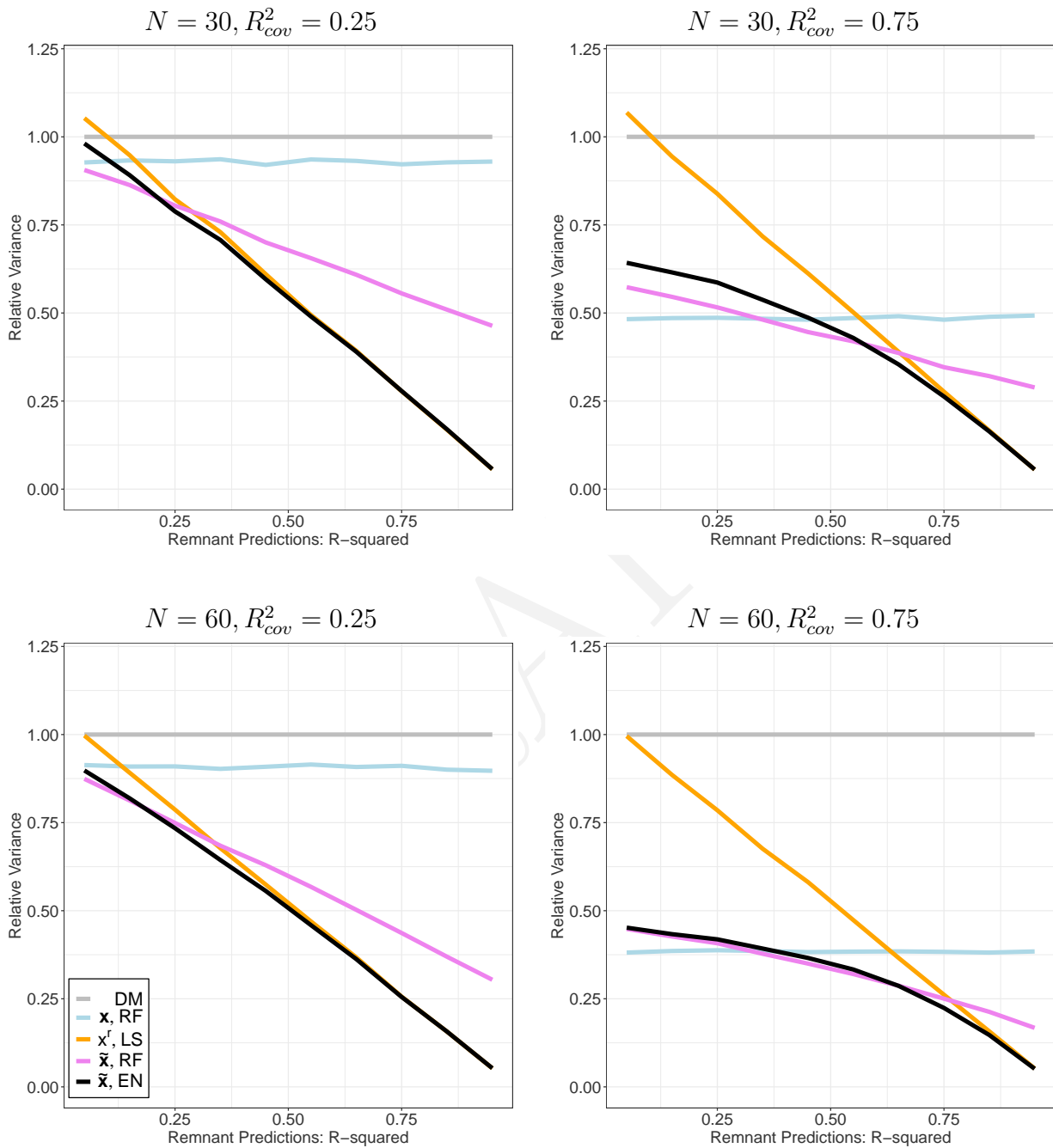


Figure 4: Varying R_{rem}^2

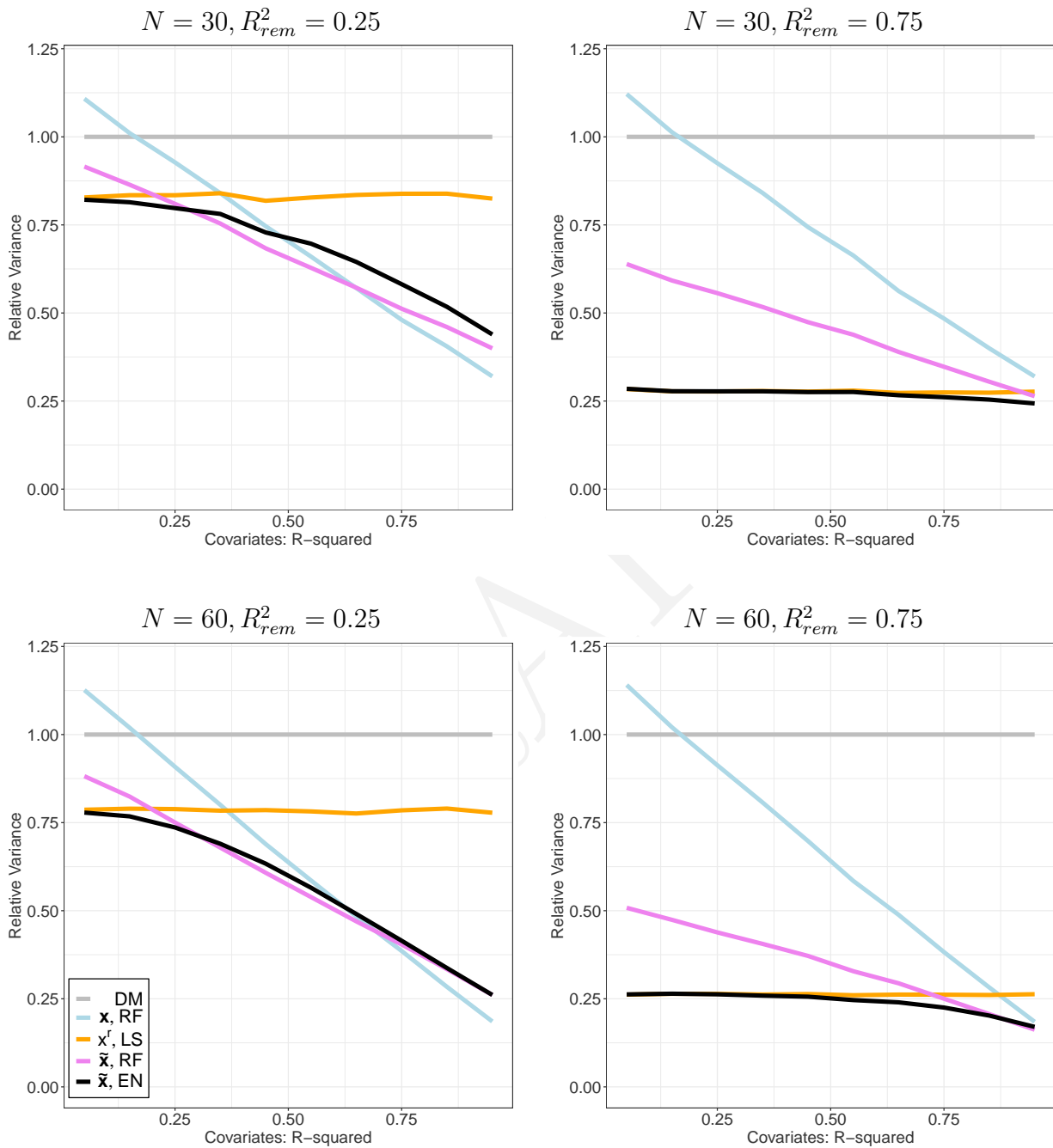


Figure 5: Varying R_{cov}^2

C Deep Learning in the Remnant to Impute Completion

We used the remnant to train a variant of a recurrent neural network [Williams and Zipser, 1989] called a Long-Short Term Memory (LSTM) network [Hochreiter and Schmidhuber, 1997] to predict students’ assignment completion. Deep learning models, and particularly LSTM networks, have been previously applied successfully to model similar temporal relationships in various areas of educational research [Piech et al., 2015, Botelho et al., 2017].

Neural networks, including recurrent networks such as those explored here, are universal function approximators [Hornik et al., 1989, Schäfer and Zimmermann, 2006]. These models are commonly represented as “layers” of neurons; these feed from a set of inputs, through one or more “hidden” layers, to an output layer, where, in the basic case, the output of each layer is determined by Equation 26. In that equation, W is a set of learned weights, comparable to the coefficients learned in a regression model. The activation function $a(\cdot)$ is commonly a non-linearity that is applied to each layer in the network.

$$h_\ell = a(W * h_{\ell-1} + b) \tag{26}$$

where h_0 is the input vector X .

Recurrent networks build upon this formulation to add layers that utilize not only the outputs of preceding layers, but also incorporate values from previous time steps within a supplied series; in time series data, the model estimates for a particular time step may be better informed by information from previous time steps, and a recurrent network structure is designed to take advantage of this likelihood. The LSTM networks explored here incorporate a set of “gates” that regulate the flow of data from both preceding layers and a “cell memory” that is calculated through previous time steps. The output of this LSTM layer is given by Equations 27-32.

$$f_t = \sigma(W_f * [h_{t-1}, x_t] + b_f) \tag{27}$$

$$i_t = \sigma(W_i * [h_{t-1}, x_t] + b_i) \tag{28}$$

$$o_t = \sigma(W_o * [h_{t-1}, x_t] + b_o) \tag{29}$$

$$\tilde{C}_t = \tanh(W_C * [h_{t-1}, x_t] + b_C) \tag{30}$$

$$C_t = f_t * C_{t-1} + i_t * \tilde{C}_t \tag{31}$$

$$h_t = o_t * \tanh(C_t) \tag{32}$$

where t is given as recurrent layer ℓ on the given timestep.

In the above equations, gates f_t and i_t inform the cell memory C_t how much of the previously-computed memory should be forgotten and updated with the output of the previous time step and preceding layer, respectively.

As a recurrent network, the model is trained by iteratively updating the weight matrices (W in the above equations) through a procedure known as backpropagation through time

[Werbos, 1990] combined with a stochastic gradient descent method called Adam [Kingma and Ba, 2014]. These methods are informed by a cost function (sometimes called a loss function) that is calculated through the comparison of model predictions with supplied ground truth labels. In this work, we adopted a network structure that incorporates multi-task learning [Caruana, 1997] as a means of regularization. In other words, our model ultimately produces two sets of predictions corresponding with two outcomes of interest: student completion and inverse mastery speed, each on the subsequent assignment. By optimizing model weights in regard to these two outcomes, the process helps prevent the model from overfitting to either outcome; as student completion of their next assignment is the outcome explored in this work, the second outcome of inverse mastery speed is used only for this regularization purpose and is not utilized in subsequent analyses. Given that student completion is binary and inverse mastery speed is a continuous measure, the formula of which is described in Table C, the cost function for our model training was calculated as a linear combination of two separate cost functions. Binary cross-entropy is used in the case of next assignment completion, as shown in Equation 33, while RMSE (Equation 34) is used in the case of inverse mastery speed on the next assignment. The final cost function is then given as Equation 35, which is calculated over smaller smaller “batches” of samples over multiple training cycles known as epochs.

$$\text{BCE} = -(y * \log(\hat{y}) + (1 - y) * \log(1 - \hat{y})) \quad (33)$$

$$\text{RMSE} = \sqrt{\frac{1}{n} \sum (y - \hat{y})^2} \quad (34)$$

$$\text{Cost}_{\text{batch}} = \frac{\text{BCE}_{\text{batch}} + \text{RMSE}_{\text{batch}}}{2} \quad (35)$$

The training of the model continues by calculating the cost and iteratively updating model weights over multiple epochs until a stopping criterion is met. In this regard, we hold out 30% of the training data as a validation set. Model performance is calculated on this validation set after each epoch of training. Training ceases once the model performance on this validation set stops improving (i.e., the difference of model performance from one epoch to the next falls below a designed threshold). To avoid stopping the training process too early due to small fluctuations in model performance on the validation set early in the training procedure, a 5-epoch moving average of validation cost is used as the stopping criterion.

The specific model structure used in this work observed an LSTM network comprised of 3 layers. We used 16 covariates to describe each single time step, which then feeds into a hidden LSTM layer of 100 nodes, which is used to inform an output layer of two units corresponding with the previously described two outcomes of interest. The input features used in this model, described in Table C, represent transformed and non-transformed versions of several metrics that describe different aspects of student performance within a single assignment. We considered sequences of at most ten worked skill builder assignments (c.f. Section 4.1), to predict student completion on a subsequent skill builder assignment.

We specified the LSTM model’s hyperparameters (e.g., number of LSTM nodes, delta of stopping criterion, weight update step size) based on previously successful model structures and training procedures within the context of education. We evaluated the model using a

Input Feature	Description
Problems Started	The number of problems started by the student. (Untransformed & Sq.Root)
Problems Completed	The number of problems completed by the student. (Untransformed & Sq.Root)
Inverse Mastery Speed	The inverse of the number of problems needed to complete the mastery assignment, or 0 where the student did not complete. (Untransformed & Sq.Root)
Percent Correct	The percentage of problems answered correctly on the first attempt without the use of hints. (Untransformed & Sq.Root)
Assignment Completion	Whether the current assignment was completed by the student.
Attempts Per Problem	The number of attempts taken to correctly answer each problem. (Avg. & Sq.Root)
First Response Time	The time taken per problem before making the first action. (Avg.)
Problem Duration	The time, in seconds, needed to solve each problem. (Avg.)
Days with Activity	The number of distinct days on which the student worked on each problem in the assignment. (Avg.)
Attempted Problem First	Whether, on each problem, the first action was an attempt to answer (as opposed to a help request). (Avg.)
Requested Answer Hint	Whether, on each problem, the student needed to be given the answer to progress. (Avg.)

10-fold cross validation within the remnant to gain a measure of model fit (leading to an ROC area under the curve of 0.82 and root mean squared error of 0.34 for the dependent measure of next assignment completion). After this evaluation, the model is then re-trained using the full set of remnant data. This trained model is then used within the analyses described in Section 4.